WAVE-RELATED DISTURBANCES IN THE VELOCITY FIELD OVER OCEAN WAVES

Stanley Paul Thompson

DUDLEY KNOX LIBRARY
NAVAL POSTGRADUATE SCHOOL
MONTEREY, CALIFORNIA 93943-5002

NAVAL POSTGRADUATE SCHOOL
Monterey, California

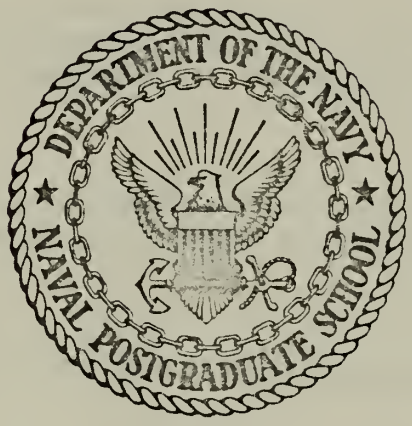

THESIS

Wave-Related Disturbances in
the
Velocity Field over Ocean Waves

by

Stanley Paul Thompson

Thesis Advisor: K. L. Davidson

September 1972

T148503

Approved for public release; distribution unlimited.

Wave-Related Disturbances in the Velocity Field over Ocean Waves

by

Stanley Paul Thompson
Lieutenant Commander, United States Navy
B.B.A., University of Minnesota, 1959

Submitted in partial fulfillment of the
requirements for the degree of

MASTER OF SCIENCE IN METEOROLOGY

from the

NAVAL POSTGRADUATE SCHOOL
September 1972

Thesis
T437
c.1

ABSTRACT

Velocity fluctuations over ocean waves and wave heights are examined using joint probability density function-conditional mean function (JPDF-CMF) analyses. Results are compared with theoretical predictions from wind-wave coupling models which provide for interaction between the wave induced motion and turbulence in the airflow, and also with predictions from potential flow theory.

Phase and amplitude results for wave-related fluctuations are examined in detail and consistent departures from potential flow are noted. These departures are phase differences in between u and w which are not in quadrature, amplitudes of u and w which vary throughout the periods, and phase shifts of u and w which differ from those predicted by potential flow theory.

Conclusions for the role of turbulence in the interactions are based on JPDF-CMF and phase amplitude analyses.

TABLE OF CONTENTS

I. INTRODUCTION ---------- 8

II. ASPECTS OF THEORETICAL AND OBSERVATIONAL RESULTS ---------- 14

A. DISCUSSION OF WIND-WAVE COUPLING THEORY --- 15

B. STATISTICAL CONSIDERATIONS AND PROCEDURES - 19

1. Preliminary statistics computation and normalization ---------- 19

2. Band Pass Filtering ---------- 20

3. JPDF-CMF Computations ---------- 21

4. Phase-amplitude theory and computation- 21

III. DESCRIPTION OF MEASUREMENTS ---------- 26

A. FLOATING INSTRUMENT PLATFORM (FLIP) ------- 26

B. EQUIPMENT AND PROCEDURES ---------- 28

1. Sensor Mounting Arrangement ---------- 28

2. Wind Component Measurement ---------- 29

3. Wave Measurement ---------- 31

IV. PRESENTATION OF RESULTS ---------- 32

A. PERIOD 1 ---------- 35

B. PERIOD 2 ---------- 44

C. PERIOD 3 ---------- 53

D. PERIOD 4 ---------- 61

V. SUMMARY AND CONCLUSIONS ---------- 71

BIBLIOGRAPHY ---------- 72

INITIAL DISTRIBUTION LIST ---------- 74

FORM DD 1473 ---------- 76

LIST OF TABLES

I. Observed and Predicted Velocity Components, and Statistical Eddy Periods for each Variable ---------- 25

II. General Conditions for Periods Analyzed -------- 34

LIST OF FIGURES

1. Side and Top View of FLIP ---------- 11

2. BOMEX and FLIP Location During 19-28 May 1969 -- 12

3. Streamlines of Sinusoidal Perturbations in a Shear Flow Near the Critical Level ---------- 16

4. Phase-Amplitude Relations Predicted by Potential Flow Theory for the Two Components of Velocity (u and w) and the Stress uw, with Respect to the Wave ---------- 17

5. Numerical Inverse Transform Filter ---------- 20

6. Two-Dimensional JPDF-CMF Array ---------- 22

7. Sensor Locations on FLIP ---------- 27

8. Three-Sensor Hot Film Probe. A Millimeter Scale is Shown on the Left ---------- 30

9. Measurements and Wind and Wave Conditions ------ 36

10. JPDF-CMF Patterns for Potential Flow ---------- 37

11. JPDF-CMF Patterns for Period 1, Subset 1 ------- 39

12. Spectral Results (Period 1) Including Covariance Spectra and Wave Spectra ---------- 41

13. JPDF-CMF Patterns for Period 1, Subset 3 ------- 42

14. Phase-Amplitude Results (Components) for Period 1, Subset 2 ---------- 43

15. Phase-Amplitude Results (Components) for Period 1, Subset 4 ---------- 45

16. JPDF-CMF Patterns for Period 2, Subset 4 ------- 46

17. Spectral Results (Period 2) Including Co-Variance Spectra and Wave Spectra ---------- 47

18. Phase-Amplitude Results (Stresses) for Period 2, Subset 1 ---------- 49

19. Phase-Amplitude Results (Stresses) for Period 2, Subset 2 ---------- 50

20. Phase-Amplitude Results (Stresses) for Period 2, Subset 3 ---------- 51

21. Phase-Amplitude Results (Stresses) for Period 2, Subset 4 ---------- 52

22. JPDF-CMF Patterns for Period 3, Subset 1 ------- 55

23. Spectral Results (Period 3) Including Co-Variance Spectra and Wave Spectra ---------- 56

24. JPDF-CMF Patterns for Period 3, Subset 3 ------- 57

25. Phase-Amplitude Results (Components) for Period 3, Subset 2 ---------- 59

26. Phase-Amplitude Results (Stresses) for Period 3, Subset 1 ---------- 60

27. JPDF-CMF Patterns for Period 4, Subset 1 ------- 62

28. JPDF-CMF Patterns for Period 4, Subset 3 ------- 63

29. Phase-Amplitude Results (Components) for Period 4, Subset 1 ---------- 64

30. Phase-Amplitude Results (Components) for Period 4, Subset 3 ---------- 66

31. Phase-Amplitude Results (Stresses) for Period 4, Subset 1 ---------- 67

32. Phase-Amplitude Results (Stresses) for Period 4, Subset 2 ---------- 68

33. Phase-Amplitude Results (Stresses) for Period 4, Subset 3 ---------- 69

ACKNOWLEDGEMENTS

The author wishes to take this opportunity to express his appreciation to his advisor, Professor K. L. Davidson, for his support, advice, and guidance throughout this research.

Appreciation is also expressed to Professor R. T. Williams for his careful review of the manuscript and useful suggestions, to Lieutenant Commander G. S. Bingham for spectral results, and to Miss Sharon Raney, Staff Programmer, for her guidance in computer programming.

The research was made possible by the Office of Naval Research through Contract N00014-67-A-0181-0005 with the University of Michigan and Task NR 083-265 with the Naval Postgraduate School. Numerical calculations were performed by computer facilities at the University of Michigan and the Naval Postgraduate School. The manuscript was typed by Miss Marion Marks.

Finally, but most importantly, to my wife Patricia, for her understanding of many months of separation, and to my children who had only a weekend father, a very grateful, thank you.

I. INTRODUCTION

More detailed studies of the near atmospheric boundary layer structure and energy exchanges are necessary if solutions to several applied geophysical problems are to be solved. Some of these applied geophysical problems include: the forecasting of surface wave conditions which require wind speeds at specified layers in the surface layer for semi-empirical formulae, and specifications of kinetic energy losses and thermal energy gains in the surface layer that are necessary for extended period weather predictions.

Previous methods for obtaining boundary fluxes and determining the structure of the air layer near the ocean surface consisted primarily of applying empirical relationships, which have been found to be valid over land. These previous efforts generally made use of the assumption that interactions associated with wind-wave coupling are negligible.

An example of the need for a better understanding of the atmospheric boundary layer structure was the discrepancies in the interpretations of results presented at the Conference on the Interaction of the Sea and Atmosphere at Fort Lauderdale, Florida in December 1971. Various results were marked by conflicting interpretations when examined with strictly empirical approaches. Most evident in these were the various representations and values obtained for the drag coefficients as well as differences from intercomparisons

between stress estimates obtained from different methods. The basic assumptions in obtaining these results were the form of the wind profile and neglect of significant dependence on the waves. General descriptions of the influence of wind-wave coupling within the framework of theoretical models combined with observational data should yield results which delineate reasons for these discrepancies.

It is appropriate to perform detailed analysis of velocity fluctuations over natural waves at this time not only because of the need to consider the dynamics of wind-wave coupling to explain discrepancies among results but also because of the present stages in both theoretical and observational efforts in this area. Recent advances in theoretical and observational studies have brought both to the point where the results should and can be related.

Theoretical studies on wind-wave coupling have progressed from the initial quasi-laminar descriptions (see Miles 1957) wherein the wave-induced motion interacts only with the mean wind to those wherein interaction occurs with the turbulence in the airflow (Yefimov 1970). Solutions from theoretical models which allow for turbulence in the airflow have revealed several features recently observed in results obtained over natural waves. These features include amplitude and phase variation of the wave-related fluctuations with height and contributions by the wave-induced motion to the cospectra of u and w. Similarities in these results suggest that theoretical models could be

refined and the observational results interpreted better if the two types of results were intercompared.

In this study, velocity fluctuations over natural waves will be examined in order to show that the airflow does not necessarily follow the potential flow definition inherent in early wind-wave coupling models. For this, recent theories and discussions of wind-wave coupling will also be considered. These include those by Yefimov (1970), Manton (1971), Davis (1972), and Davidson (1970).

The data examined represent simultaneous velocity measurements at different levels over ocean waves on the Atlantic Ocean. The measurements were made from the Scripps Institution of Oceanography Floating Instrument Platform (FLIP) which appears in Figure 1. The measurements were made during the Barbados Oceanographic and Meteorological Experiment (BOMEX). The BOMEX experiment was a joint investigation of several agencies and universities for the purpose of establishing the energy budget of an atmospheric volume 500 km on a side and about 5 km high. The volume was located in the Trade Wind region of the Atlantic Ocean as shown in Figure 2. The data represent measurements near the center of the volume, in the vicinity of 16^{o}N latitude and 57^{o}W longitude.

In this study, joint probability analysis on velocity and wave are the primary source for information on interactions that could have taken place due to wind-wave

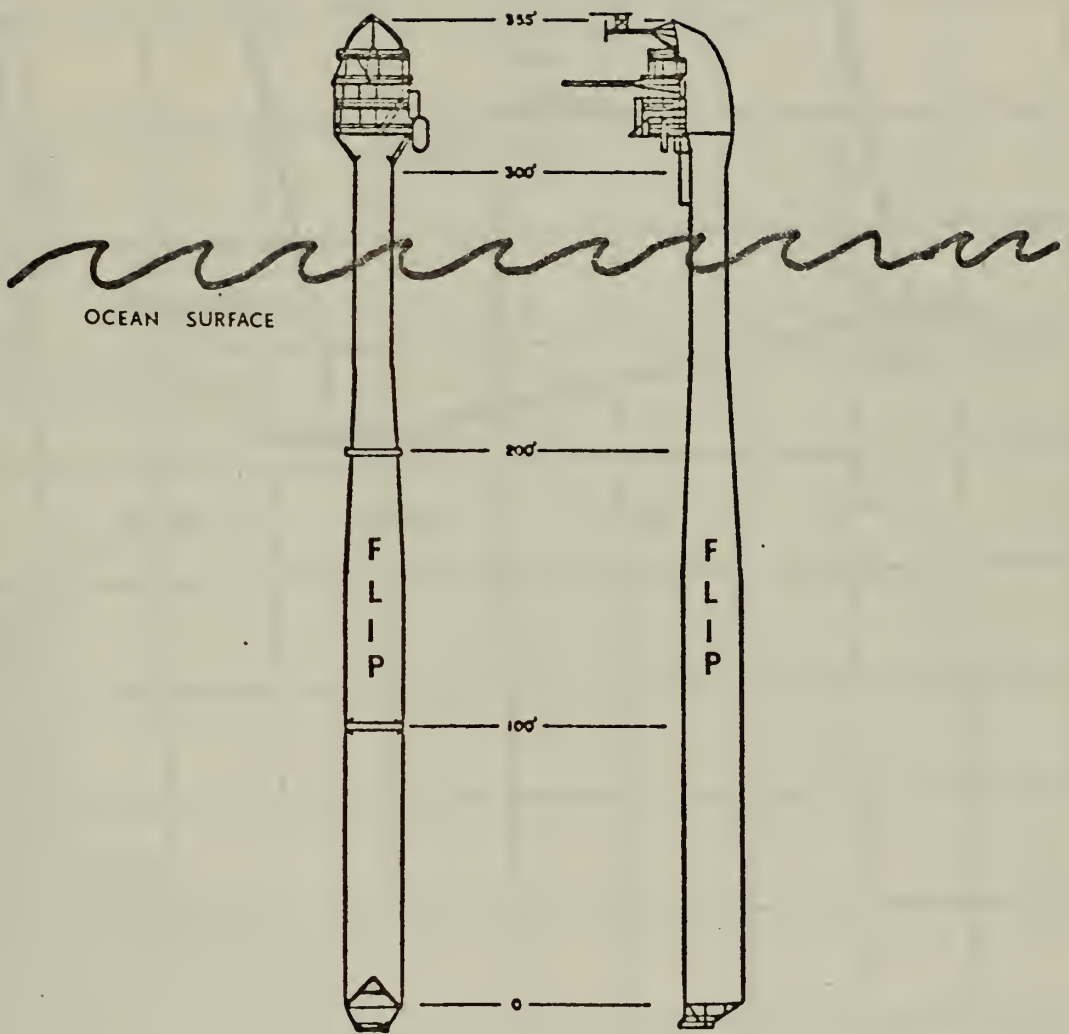

Figure 1. Side and Top View of FLIP.

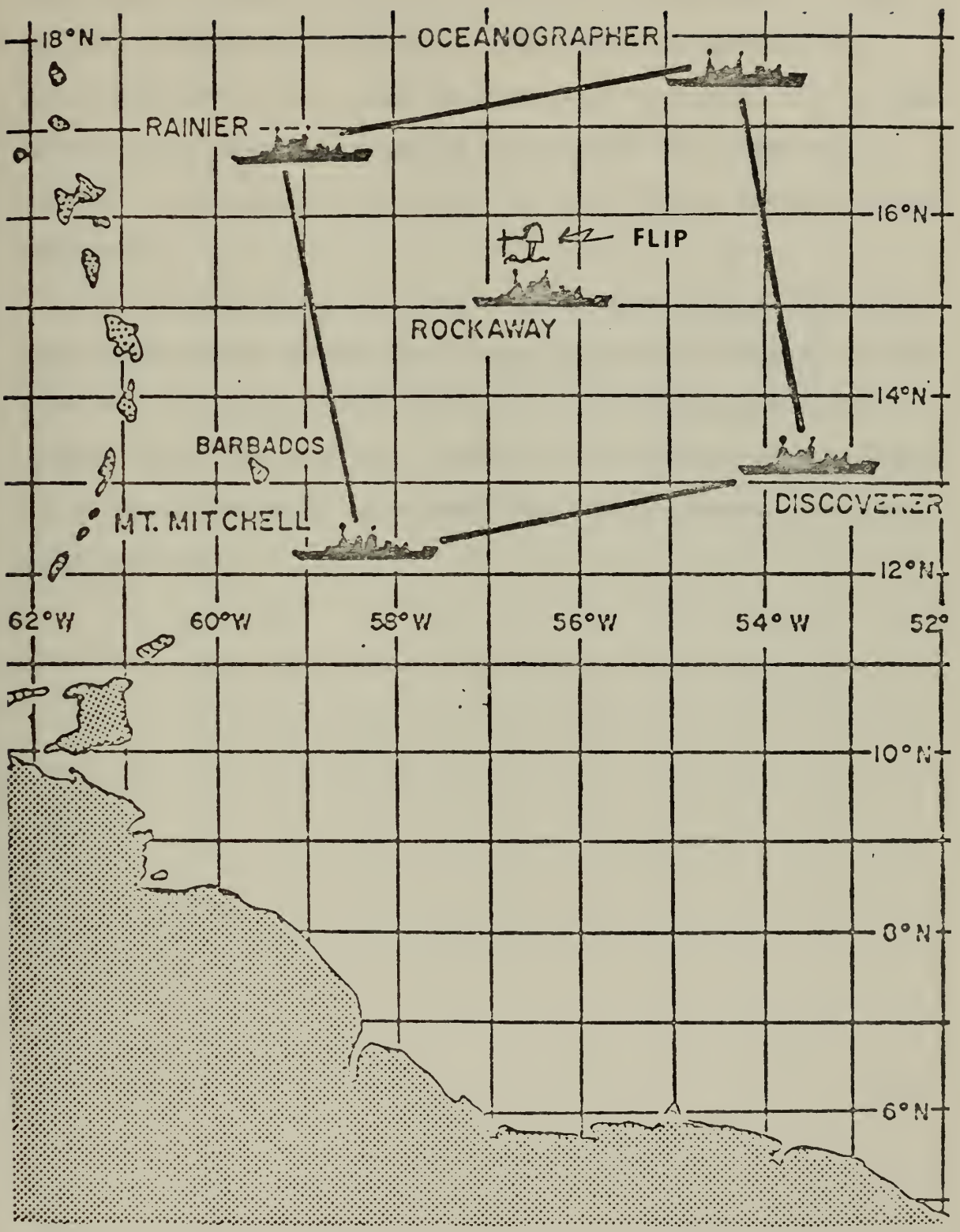

Figure 2. BOMEX and FLIP Location During 19-28 May 1969.

coupling. From the analyses, interpretations will be made on phase-amplitude relations, non-linear properties and determination of the type of turbulence present. It is suggested that these statistical procedures will find widespread acceptance in the study of micro-scale meteorological phenomena.

Data examined in this study were also analyzed by spectral analyses in a parallel investigation by Bingham (1972). Some of his results will be referenced during the discussions. Spectral analysis, however, is limited when applied to studies involving phase-amplitude relationships between wind and wave.

II. ASPECTS OF THEORETICAL AND OBSERVATIONAL RESULTS

A primary motivation for the design of this investigation was the close agreement between recent observational results and numerical solutions from recent wind-wave coupling models by Yefimov (1970) and Reynolds (1968). In formulating their models, Yefimov and Reynolds allowed for interaction between the wave-induced motion and the turbulence in overlying shear flow. Although most theoretical formulations of the linear theory for wind-wave coupling have several common assumptions; such as, two dimensional flow and a specified mean wind dependent only on height, and common simplifications; such as a single component wave field and suitable linearized forms for the defining equations, a distinguishing feature of recent formulations has been the role prescribed for turbulence in the airflow. In contrast, Miles (1957), in formulating an early quasi-laminar model, neglected turbulence except for its role in determining an assumed logarithmic mean profile.

Davis (1972) has shown that anistropic stresses, which are most likely to be turbulent Reynolds stresses, are essential to the process of energy flow to the wave. These stresses, however, have been difficult to isolate in the various experimental tests of the models. Careful measurements and improved analyses of the fluctuating velocity components and the turbulent stresses are apparently what are required.

A. DISCUSSION OF WIND-WAVE COUPLING THEORY PREDICTIONS

Miles' theory is a quasi-laminar wave generation mechanism in which the wave-related motion is assumed to follow the potential flow theory. The key to Miles' formulation is the existence of the critical level which corresponds to the level where the wind speed is equal to the wave speed. A schematic of Miles' assumed airflow is shown in Figure 3. The wave in this figure is stationary. Below the critical level (dotted line), the air appears to move to the left since it moves at a slower speed than the waves. Above the critical level, the wind moves to the right. Miles' theory is based on the premise that waves only modulate the mean wind flow over them and that turbulence is not influenced. Reynolds stresses are then dependent only on the height above the mean wave surface. Phase and amplitude features of the two components of velocity, and the stress uw, with respect to the wave, as predicted by potential flow theory are illustrated in Figure 4.

Recently, Yefimov (1970) and others have allowed for turbulence in the airflow, which requires taking into account nonlinear terms in the equations of motion. A way to approach this has been to define the total vertical transfer of horizontal momentum as, (Yefimov 1970),

$$-u'w' = k_m \frac{\partial \bar{u}}{\partial z} + \gamma\left(\frac{\partial u}{\partial z} + \frac{\partial w}{\partial z}\right)$$

where u' and w' represent total velocity fluctuations, u and w are wave-related fluctuations, $\bar{u}$ is the mean wind, k_m =

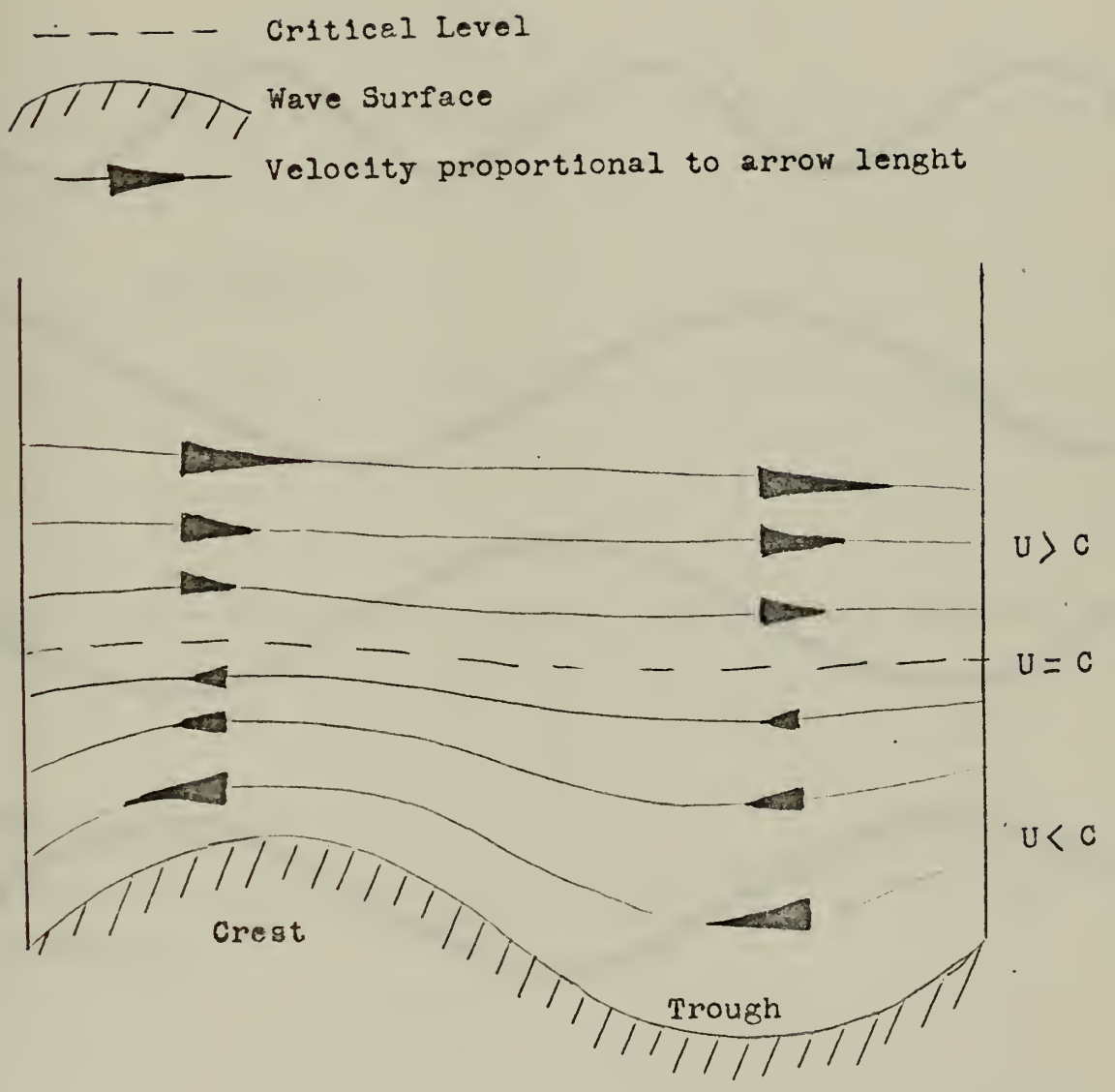

Figure 3. Streamlines of Sinusoidal Perturbations in a Shear Flow Near the Critical Level.

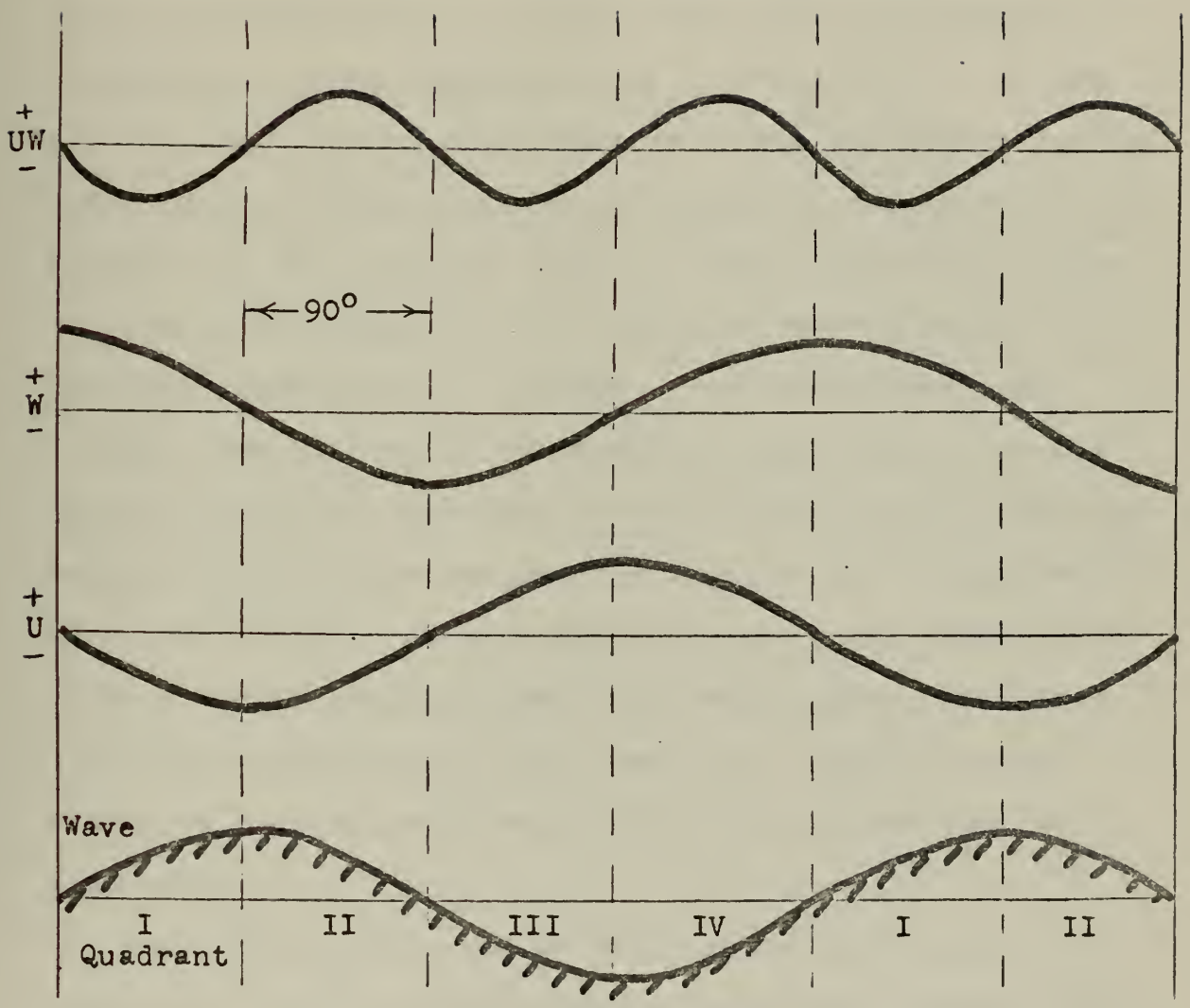

Figure 4. Phase-Amplitude Relations Predicted by Potential Flow Theory for the Two Components of Velocity (u and w) and the Stress uw, with Respect to the Wave.

ku_*z and γ is an exchange coefficient related to the wave-induced motion.

Several features in Yefimov's solutions are due solely to the prescribed interaction between the wave-induced motion and turbulence. As such, they occur independent of the height or even existence of a critical level. In comparison, all nonpotential features of the airflow in initial quasi-laminar formulations were intimately connected to the dynamics at the 'critical level'. These features were the variations with height of the phase difference between the velocity components and the wave. Phillips (1966) and Kinsman (1965) describe the predicted phase shift for the vertical velocity component as being from over the downwind node toward the crest as the 'critical level' is approached from the surface. Stewart (1969) and Reynolds (1968) were able to verify results from a wind-wave tunnel experiment with phase predictions from a nonlinear formulation for wind-wave coupling and their work will be referenced for this aspect.

Consideration of results with respect to theoretical approaches for the consequences of wind-wave coupling will be confined to prescribed or predicted characteristics of the velocity field in these models. These characteristics include:

a. Variation of the amplitude of wave-related fluctuations with height;

b. Contributions (negative or positive) to the momentum flux; and

c. Variation of the phase difference between wave-related velocity fluctuations and the wave with height.

B. STATISTICAL CONSIDERATIONS AND PROCEDURES

Both joint probability density function-conditional mean function analyses (JPDF-CMF) and spectral analyses will be used to identify properties of fluctuation velocities associated with the waves' presence but only the JPDF-CMF analyses will be described in some detail.

The following diagram outlines procedures[1] used in the JPDF-CMF analyses. The procedures will be discussed in the ensuing paragraphs.

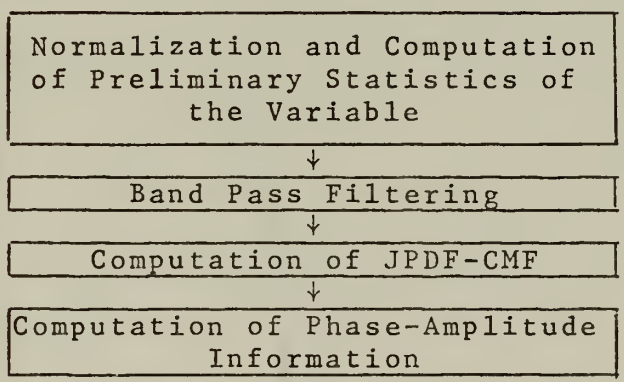

1. Preliminary Statistics Computation and Normalization

The procedures were applied to normalized values of the original data. Normalization was accomplished by

[1]All statistics were compiled and plotted at the W. R. Church Computer Facility of the Naval Postgraduate School utilizing the IBM computer and a CALCOMP plotting device.

dividing the deviation from the mean by the standard deviation; for example $(x - \bar{x})/\sigma$.

2. Band Pass Filtering

A band pass filter was applied in order to focus the analyses on fluctuations near the frequency band corresponding to predominant surface waves. Specifically, application of the band pass filter allowed analyses of wave-induced fluctuations to be clear of any high or low frequency contamination. A numerical inverse transform filter was applied and was designed on the basis of previous spectral results. The response curve for the selected band pass filter appears in Figure 5, where low and high frequency cut-offs are observed to be approximately .1 and .8 Hz respectively.

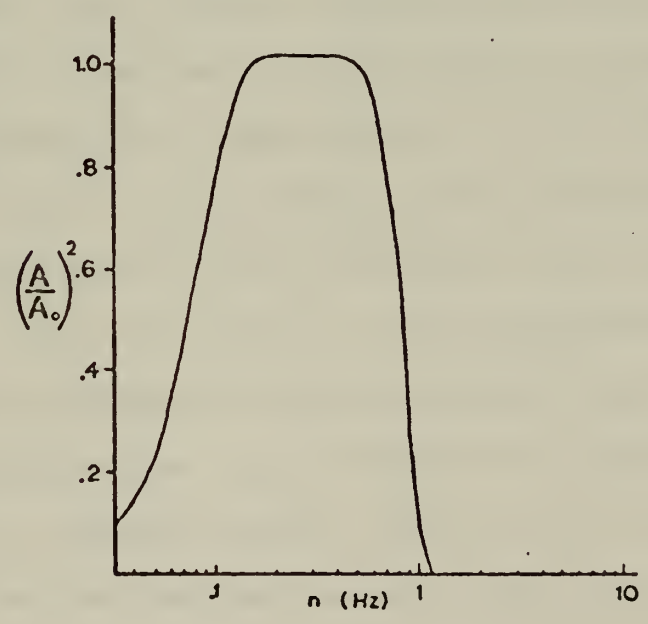

Figure 5. Numerical Inverse Transform Filter.

3. JPDF-CMF Computations

JPDF-CMF procedures adopted for this study have been fully described by Holland (1972). In general, a JPDF represents the probability of a joint occurrence for a pair of variables and the CMF represents the average value of a third variable in a joint class interval for all observation times when JPDF variables had values within the joint interval. Figure 6 shows a two-dimensional array representing the trivariate statistical relationship described by the JPDF and CMF. From this figure, the probability of joint occurrences in two variables can be compared with a corresponding conditional mean of a third variable.

4. Phase-Amplitude Theory and Computation

Available theoretical (Yefimov 1970, Manton 1971) and observational (Davidson 1970, Holland 1972, Davidson and Frank 1973) results indicate that one of the important features of interest in this type of study is the statistical dependence of fluctuations in the airflow on the phase of the wave. Such relations were determined by Davidson and Frank (1973) using procedures which are used in this study. It is in regard to phase-amplitude information that greater latitude for interpretations can be made in JPDF-CMF analyses than those obtained by spectral analyses. For example, JPDF-CMF results should reveal nonlinear features since the information is not a result of linear expansions of the fluctuations. Furthermore, the approach can be applied to comparisons between wave-amplitude classes. In

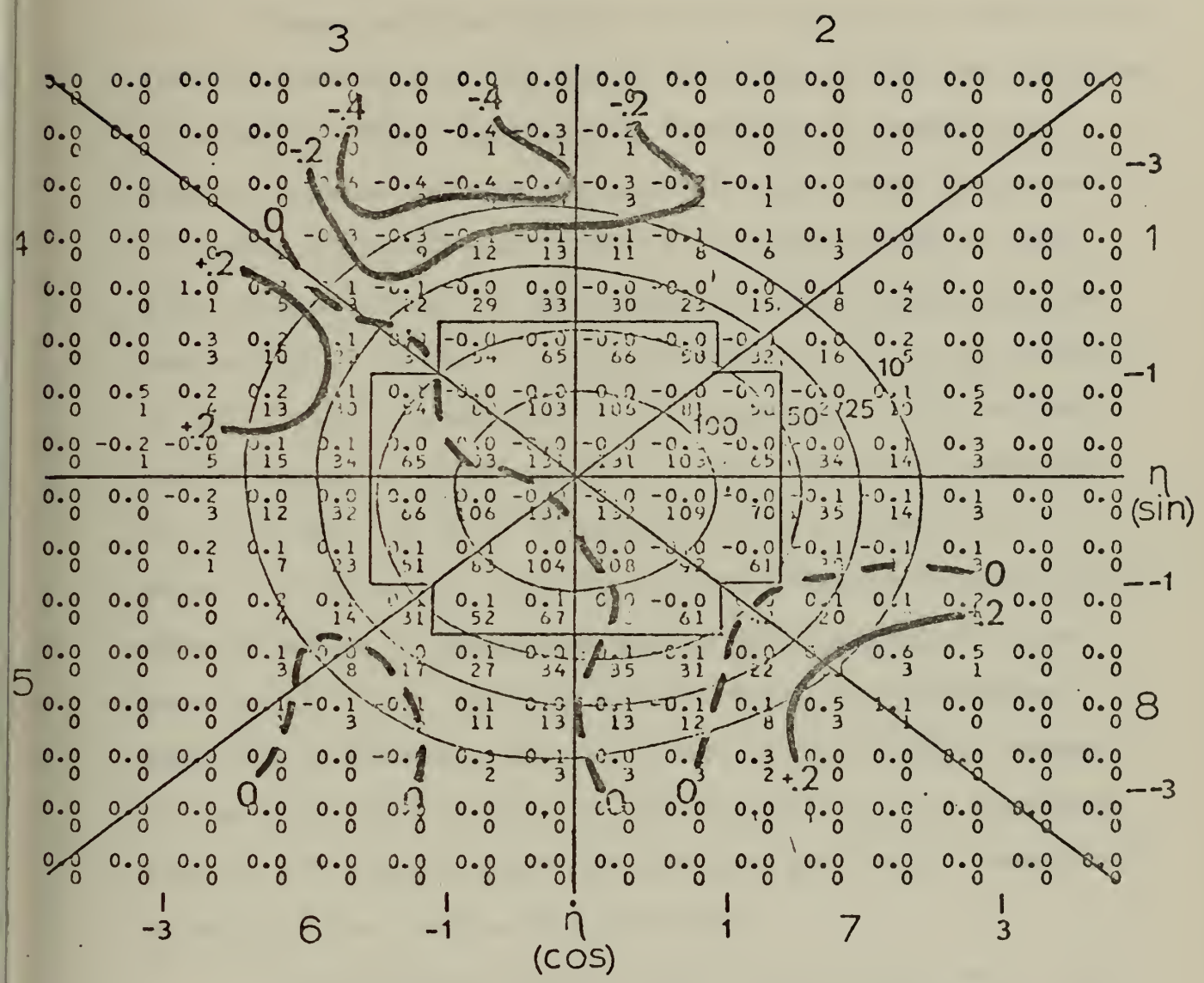

Figure 6. Two-Dimensional JPDF-CMF Array.

this study the features are examined with respect to small, large, and combined or total waves.

Phase information was determined using a method described by Holland (1972) which is based on JPDF-CMF analyses procedures. Phase-amplitude information is possible by such procedures because polar coordinates which represent the phase angle and amplitude of a variable such as the wave height (η) can be determined from the JPDF array for the variable, η, and its time derivative, $\dot{\eta}$. As an example of this, $u(\dot{\eta}, \eta)$ would show the dependence of the horizontal component of wind velocity on the phase and amplitude of the waves. As will be seen in later discussions, the phase is defined in terms of octants measured counterclockwise in the $\dot{\eta}$, η coordinate system (JPDF array) from the positive $\dot{\eta}$ axis. JPDF-CMF arrays which contain phase-amplitude information for u,v,w,uv,uw, and vw with respect to the waves will appear in the discussions of a following section. The phase-amplitude results are easily summarized by octants for each period analyzed.

In determining phase-amplitude information, a parameter, τ_o, called the 'statistical eddy period' is also of interest. τ_o is defined by the ratio

$$\tau_o = 2\pi \frac{\sigma}{\dot{\sigma}}$$

where σ and $\dot{\sigma}$ are standard deviations of the variable and its derivative. If the statistical eddy periods compared differ greatly between the independent and reference

variable, phase-amplitude information for the reference variable has a greater possibility of only representing the mean of numerous random fluctuations. In general, the statistical eddy periods agree as can be seen in Table I.

With respect to possible influence by FLIP's motion on the results, analyses by Rudnick (1967) have indicated that observed fluctuations in u and w are 10^2 times larger than could be induced by FLIP's motion. Therefore, FLIP's motion will not enter into the discussion of the results.

Table I. Observed and Predicted Velocity Components, and Statistical Eddy Periods for Each Variable.

Period	U-Component(M/Sec)			W-Component(M/Sec)			Statistical Eddy Period(τ_o)[4]						
Subset	Observed	Predicted[1]		Observed	Predicted[1]		n	u	v	w	uv	uw	vw
1-1	.14	.03[2]	.21[3]	.03	.06[2]	.17[3]	5.5	3.8	3.0	3.2	2.6	2.7	2.5
-2	.20	.04	.16	.04	.07	.13	5.5	4.0	3.6	3.2	2.9	2.7	2.6
-3	.18	.04	.18	.04	.07	.14	5.4	4.0	3.4	3.3	2.7	2.6	2.5
-4	.16	.02	.20	.03	.05	.16	5.6	3.9	3.2	3.3	2.8	2.7	2.5
2-1	.19	.06	.09	.03	.07	.07	4.8	3.9	4.1	3.2	2.9	2.8	2.8
-2	.21	.07	.08	.02	.08	.06	4.9	3.8	3.8	3.1	3.1	2.7	2.7
-3	.19	.06	.07	.03	.07	.05	4.7	3.6	3.9	3.3	2.7	2.7	2.7
-4	.21	.08	.07	.06	.09	.05	4.7	4.0	4.0	3.5	2.9	2.8	2.9
3-1	.26	.12	.28	.11	.17	.23	5.5	4.0	3.5	3.8	2.7	2.7	2.9
-2	.32	.07	.24	.15	.12	.19	5.8	4.5	3.8	3.7	2.8	3.0	2.8
-3	.30	.07	.30	.12	.11	.25	5.6	4.2	3.6	3.4	2.9	2.8	2.7
4-1	.26	-.02	.24	.10	.02	.20	5.8	4.0	3.7	3.1	2.8	2.8	2.7
-2	.20	.01	.25	.08	.04	.21	5.4	4.0	3.1	3.0	2.6	2.6	2.5
-3	.23	.00	.21	.10	.02	.17	5.4	4.0	3.2	3.0	3.1	2.7	2.9

[1] determined from the formulae: $U = [ka(\bar{u}-c)-a\frac{\partial \bar{u}}{\partial z}]e^{-kz}$, $W = [ka(\bar{u}-c)]e^{-kz}$ where $k = 2\pi/\lambda$, λ = wave length, a = amplitude, u = mean wind, c = wave phase speed

[2] $c = g/(2\pi x\eta_o)$, $\eta_o = \frac{1}{\tau_o}$, τ_o = statistical eddy period.

[3] c = speed determined by wave spectrum peak

[4] $\tau_o = 2\pi\sigma/\dot{\sigma}$

III. DESCRIPTION OF MEASUREMENTS

The data available for this study consisted of simultaneous recordings of wind velocity components (with hot-film anemometers), air temperature fluctuations and wave heights. The levels of measurement ranged from 2 to 8 meters above mean water level and the sensors and recording systems were capable of measuring velocity and temperature fluctuations of frequencies up to 50 Hz. There were about 54 hours of recordings in 40 separate observation periods to select from. On the basis of meteorological and wave conditions and on previous spectral analyses, four periods were chosen for the analyses.

In the following paragraphs specific details on the measurements and general conditions for every period will be described.

A. FLOATING INSTRUMENT PLATFORM (FLIP)

A discussion of FLIP has been provided by Bronson and Glosten (1968). The Floating Instrument Platform is a super-stable, open-sea, free-floating platform, which is towed to a site while in a horizontal position and then partly flooded to cause the structure to flip to a vertical position for use as a research platform. Figure 1 included a side and top view of FLIP, while Figure 7 illustrates the working section of FLIP which remains above the water line when FLIP is in the vertical position.

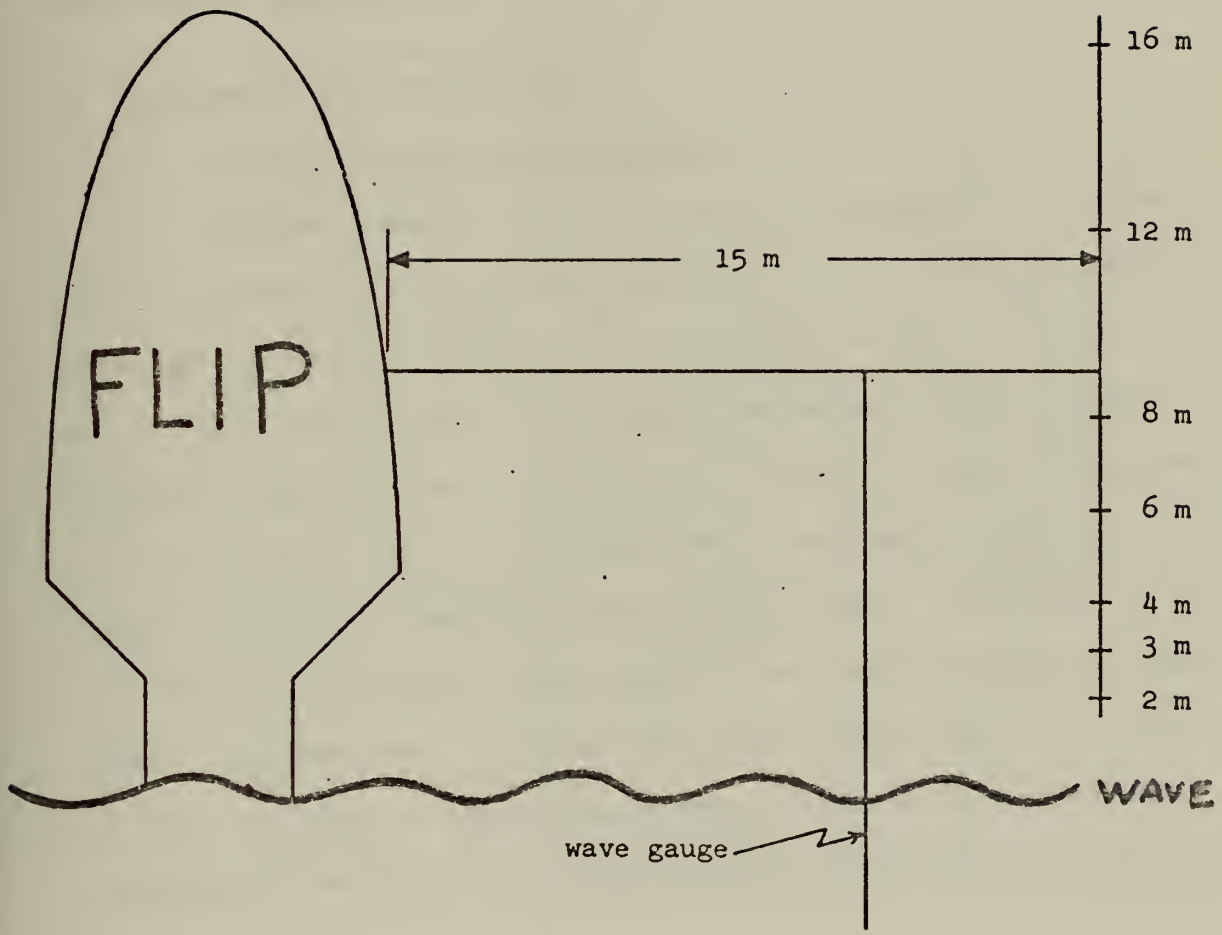

Figure 7. Sensor Locations on FLIP.

In general, FLIP performed in a satisfactory manner throughout its use in BOMEX. Wind tunnel tests revealed that a minimum distortion to the natural flow of air past the intended location of an outboard mounted vertical sensor supporting mast occurred when the deck of FLIP was positioned facing into the wind.

B. EQUIPMENT AND PROCEDURES

1. Sensor Mounting Arrangement

Figure 7 shows the locations of sensors for turbulence, profile and wave measurements on the vertical mast attached to FLIP. Sensors were mounted at the 2, 3, 4, 6, and 8 meter levels and all sensors were more than 1 meter windward from the vertical mast. As can be seen in Figure 7, the vertical mast, supported by a horizontal boom, is about 15 meters crosswind from FLIP's hull. The mast was attached to a carriage that could move horizontally on the boom. In addition, the mast could be turned on a horizontal axis so that it could be brought alongside a working platform to replace and adjust sensors during the experiment.

No provision for adjusting the vertical position of the mast, independent of FLIP, were available. This made it almost impossible to maintain sensors in a mean level position. Provisions were made, however, to correct for this discrepancy. In general, it is felt that instrument mounting arrangements have not significantly affected

the accuracy of the data values with regard to the interpretations made.

2. Wind Component Measurement

Wind components were measured with hot-film, constant temperature anemometer systems[2], with linearizers. Each probe[3] had three quartz-coated mutually perpendicular sensors 0.15 millimeter in diameter and 2.0 millimeters long. Each sensor is a glass rod covered with a platinum film onto which a quartz coating has been sputtered (see Figure 8). The sensors were electrically isolated so that simultaneous measurements could be made. The orthogonal array made it possible, with trigonometric relationships, to determine the instantaneous vector components of the wind from simultaneous measurements. The frequency response of these sensors appeared to be well over 50 Hertz in the conditions under which they were used.

The constant temperature anemometer system measures velocity by sensing the heat loss from the heated sensor to the moving air. If the air density is nearly constant and if the sensor is maintained at a constant and relatively high temperature, the heat loss is dependent almost entirely on air velocity. The sensor is part of a bridge circuit.

---

[2]Thermo-Systems, Model 1054B

[3]Thermo-Systems, Model 1294-60

Figure 8. Three-Sensor Hot Film Probe. A Millimeter Scale is Shown on the Left.

3. Wave Measurement

Wave data were obtained from a resistance gauge made available by Dr. R. E. Davis, Scripps Institution of Oceanography. The probe consisted of a non-conducting tube, approximately 2.5 centimeters in diameter, with a conducting wire wrapped spirally around it. It was positioned about 5 meters inboard from the vertical mast that held the velocity and temperature sensors.

IV. PRESENTATION OF RESULTS

The results are from four different periods. The periods were in three separate days in May 1969: 19 May (1613 -1735 GMT), 27 May (0311-0435 GMT), and 28 May (1756-1916 and 2028-2150 GMT). Each period was approximately 80 minutes in duration. Hereafter, these periods will be referred to as periods 1, 2, 3, and 4. Each period consisted of several subsets with regard to JPDF-CMF and phase-amplitude analyses; periods 1 and 2 consisted of four subsets of 20 minutes each, and periods 3 and 4 consisted of three subsets of 20 minutes each. Separate reference will be made to individual subsets within these periods when required.

Airflow data for periods 1, 2, and 4 were from the 8 meter level and those for period 3 were from the 3 meter level. Data considered were the u, v, and w velocity components and wave heights.

General conditions during the four periods are summarized in Table II and Figure 9. General conditions during all periods could be described as being steady with respect to both waves and wind. Certainly the periods did not have active wave growth or rapid decay. These conditions are representative of conditions over most of the oceans when swell propagates into regions of relatively light winds. Therefore, these results are relevant to describing the surface layer over the ocean.

Spectral results from these periods have been described by Bingham (1972). They show corresponding extrema in the velocity variance, covariance spectra and wave spectra and reflect a few characteristics of the predicted solutions, as will be noted in the results. UW cospectra had extrema which, in fact, represented either enhanced or decreased momentum transport when compared to that at frequencies not associated with wave spectra extrema. Potential flow does not predict such extrema in the uw cospectra because in theory, u and w are in quadrature. Such contributions, both negative and positive, are interpreted as being those predicted by the recent theoretical solutions.

Physical processes can be realized from the arrays representing probabilities of joint occurrences of fluctuations of various magnitudes in (u, w, uw, etc.) in conjunction with an average surface elevation during the joint occurrences.

JPDF-CMF patterns for potential flow are presented in Figure 10. As indicated in Figure 4, potential flow theory predicts a maximum positive value of uw occurring in quadrant II and IV. The JPDF-CMF pattern in Figure 10, (Panel A), represents such a relationship. Similarly, u and w relationships which appear in Figure 4 are represented in Panels B and F. Panel C and E will be discussed in the following paragraph. Panel D reflects the absence of any correlation between the CMF, v, and the JPDF ($\dot{\eta}$, η).

TABLE II. General Conditions for Periods Analyzed.

PERIOD	MEASUREMENT LEVEL (METERS)	WIND SPEED (M/SEC)	PHASE SPEED (M/SEC)	CRITICAL HEIGHT (METERS)	U_* (M/SEC)	$C - U_*$
1	8	9.7	13.9	> 15	.20	69
2	8	11.6	16.1	> 15	.28	58
3	3	10.5	15.2	> 15	.17	88
4	8	9.3	14.7	> 15	.24	62

Panel C represents the probability of joint occurrences of fluctuations of various magnitudes of u and w with respect to the wave height. The following diagram interprets the four quadrants in Panel C with respect to momentum transfer. Panel E has, of course, the CMF, wave derivative, rotated 90 degrees clockwise from its orientation in Panel C.

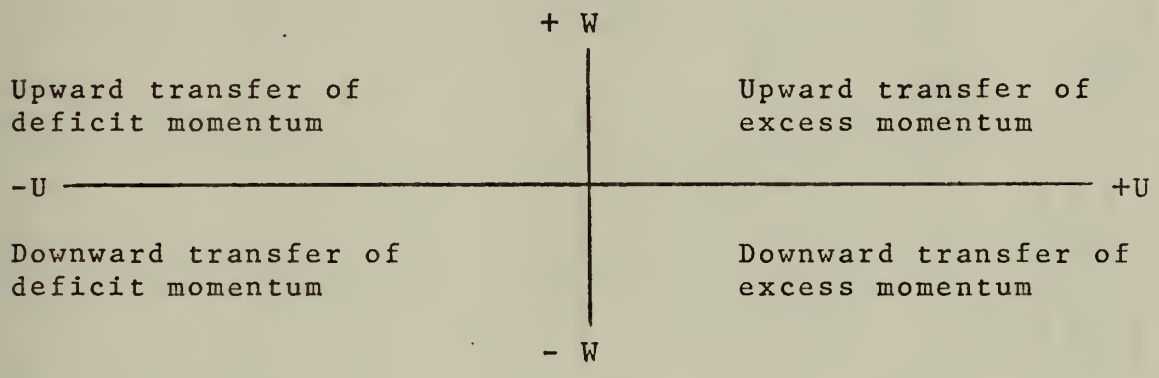

The following sections include detailed discussions of features in JPDF-CMF patterns for each of the four periods commencing with period 1 and continuing through period 4. A summary will follow the presentation of results.

A. PERIOD 1

Significant features identifiable within JPDF-CMF results from this period are evidence of mechanical turbulence associated with hydrostatic stability, decreased momentum transfer due to the waves' presence, large deviations from potential flow and apparent changes in u and w phase relations with respect to the wave due to height variations of the critical level.

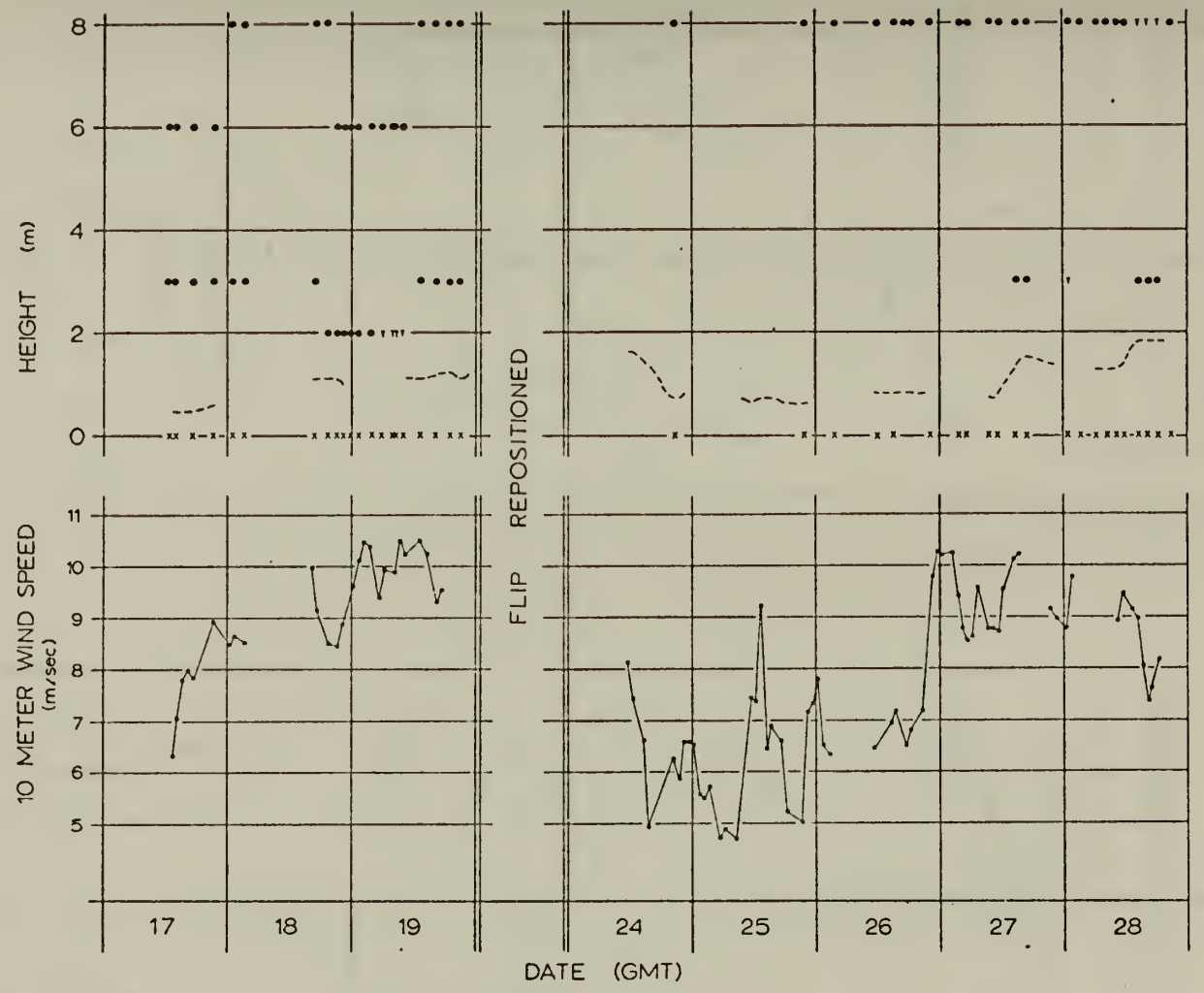

Figure 9. Measurements and Wind and Wave Conditions.
Upper half: The symbols and letters show heights and times of University of Michigan measurements aboard FLIP.
. - u,v,w,T; T - T only; x - waves; ----- - visual estimates of wave heights.
Lower half: Average wind speed at 10 meters.
(From Portman et al 1970).

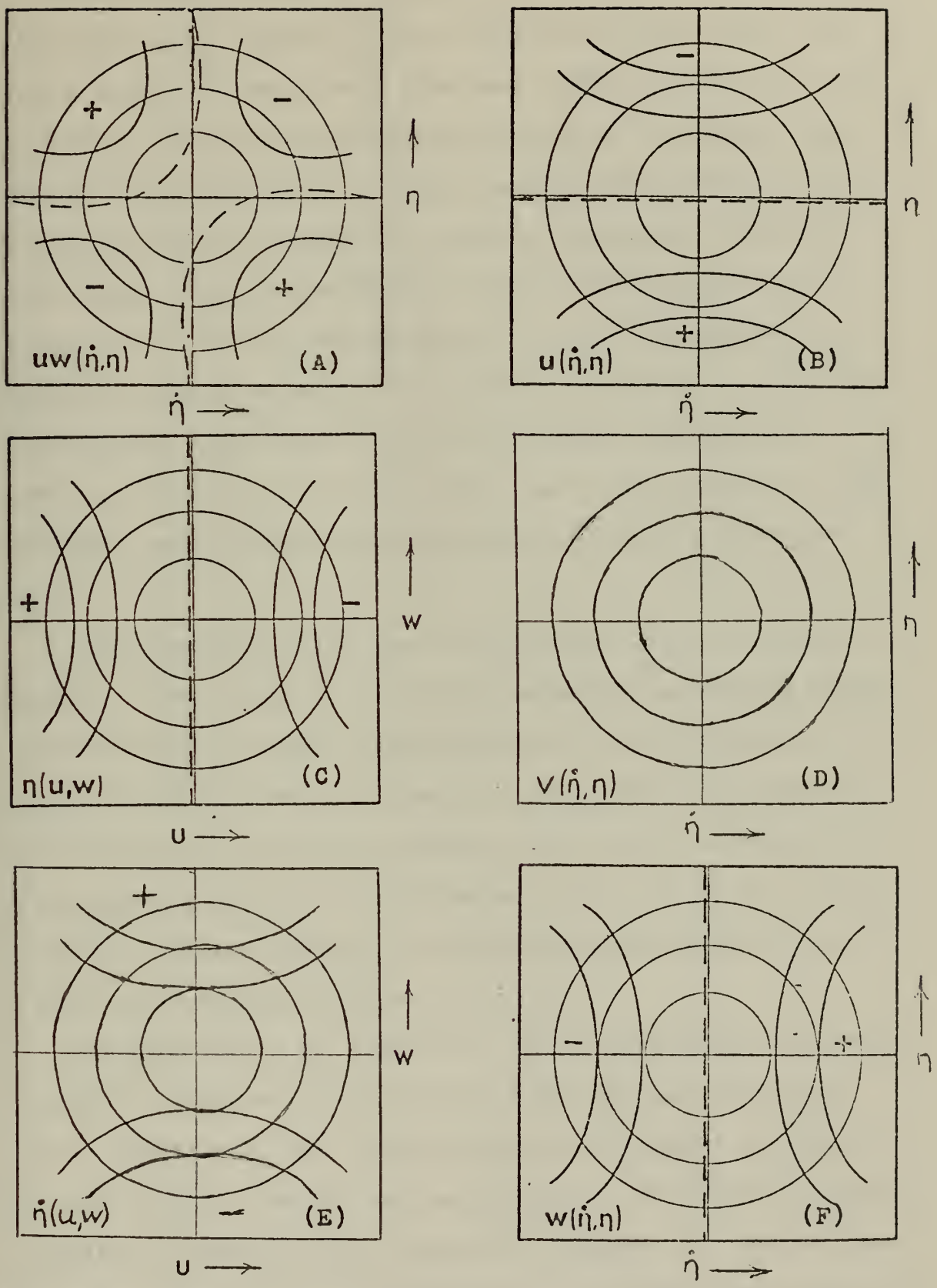

Figure 10. JPDF-CMF Patterns for Potential Flow.

With regard to the evidence of mechanical turbulence, the JPDF (u,w) patterns can be interpreted for these features in the fluctuations. Holland (1968) proposed that if turbulence is primarily mechanical and is occurring under stable conditions then a wider distribution of both u and w should occur at positive u than at negative u and the main mode, at high probability should be shifted towards negative u. Distributions which fit such a description appear in the JPDF pattern in Figure 11, Panel C. If the hydrostatic conditions had been unstable, the opposite effect, a narrow distribution of u and w at positive u and the main mode shifted towards positive u would have been seen.

JPDF patterns below the 5 percentage level in Figure 11, (Panel C) are slightly elliptic, asymmetrical with a major axis 135 degrees counterclockwise from the positive u-axis. Statistically, a small probability of joint occurrences of fluctuations of various magnitude of u and w is observed in quadrants II and IV, indicating that, due to the waves' presence, upward transfer of deficit momentum and downward transfer of excess momentum occurred.

From cospectra in Figure 12, it is observed that upward transfer of momentum was evident near the wave spectra peak. Similarly, the center patterns in Figure 11 (Panel C) are nearly circular and correspond to decreased downward transfer as shown in the cospectra, Figure 12. Recall that in these interpretations the band-pass filter (see Figure 5)

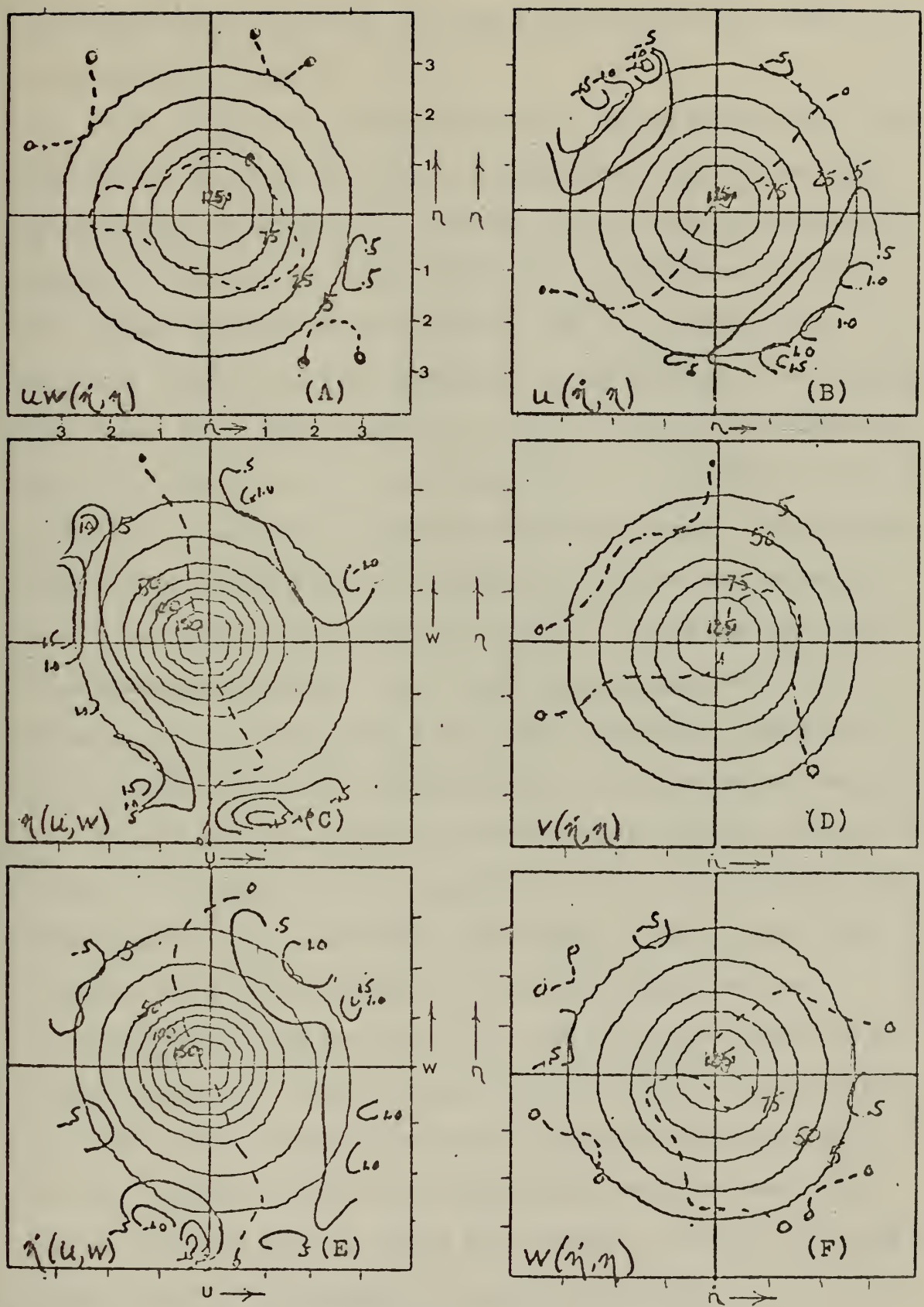

Figure 11. JPDF-CMF Patterns for Period 1, Subset 1.

included frequencies of a greater range than the wave spectra peak band.

With respect to phase relations, large deviations from potential flow can be noted by comparing $u(\dot{\eta}, \eta)$ and $w(\dot{\eta}, \eta)$ patterns of Figure 13, (Panels B and F) with comparable panels in Figure 10. In particular, a rotation of about 45 degrees is seen in the CMF of $u(\dot{\eta}, \eta)$. This is an obvious shift from that predicted by potential flow (Figure 10, Panel B). CMF patterns in $w(\dot{\eta}, \eta)$ are not as dominant as the patterns to be considered later for period 3, yet a rotation of about 45 degrees can be discerned. The phase-amplitude relationship in Figure 14 further reflects the above deviation from potential flow. The phase-amplitude representation shows w to be nearly in-phase with the u component. In contrast, potential flow theory predicts that u and w will be in quadrature as was shown in Figure 4.

Karaki and Hsu (1968) observed phase results similar to those just described by comparing u and w perturbation over water waves in a laboratory experiment. These were observed, from their analysis, near the region of the critical level and were due to a shift in the phase of w relative to both the wave phase and u-phase. The relative u-w phase was observed to be near zero in the critical level. Stewart (1970) also described results where the phase shift of both u and w with height resulted in u and w being out of quadrature and nearly in-phase.

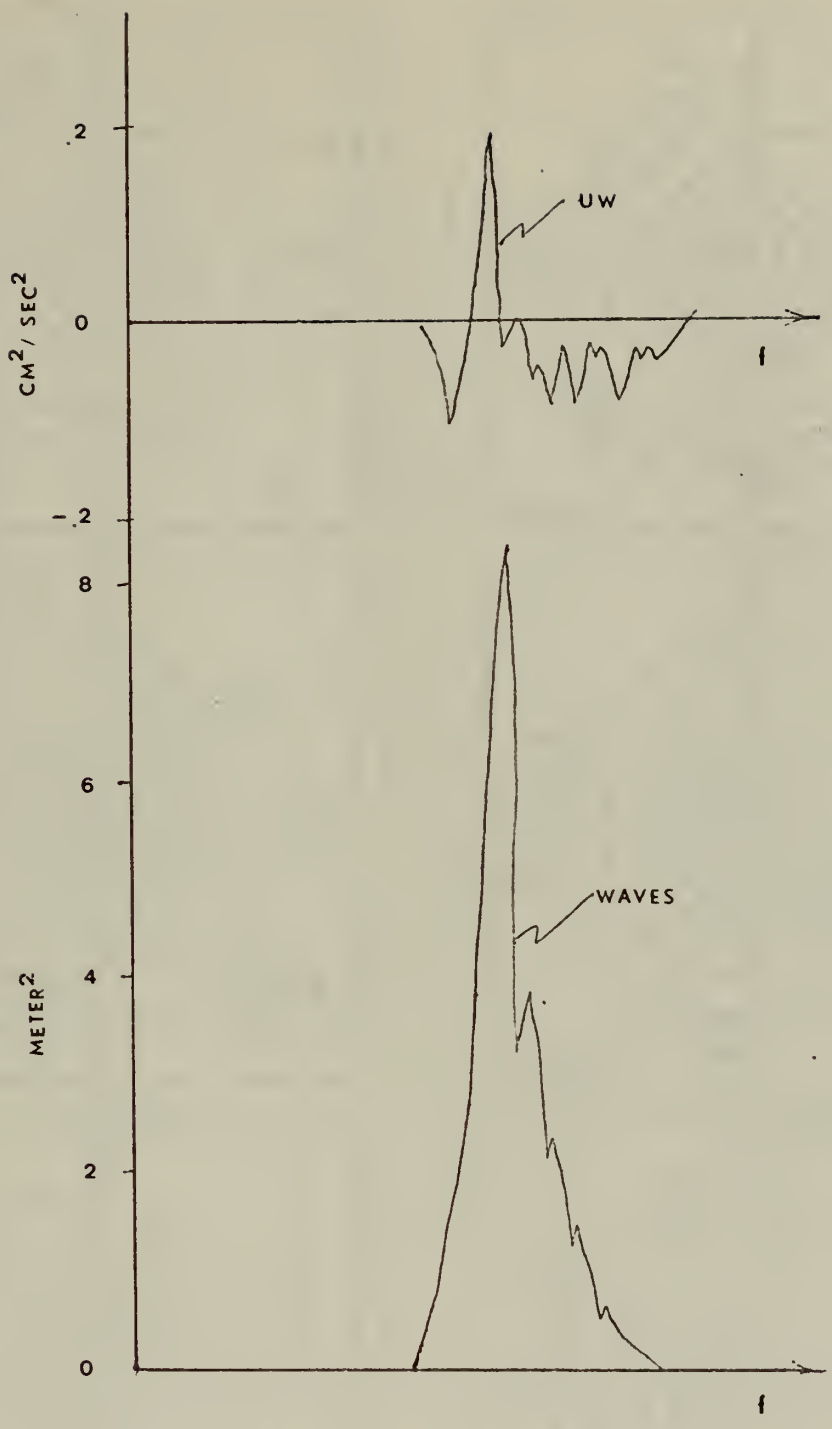

Figure 12. Spectral Results (Period 1) Including Covariance Spectra and Wave Spectra.

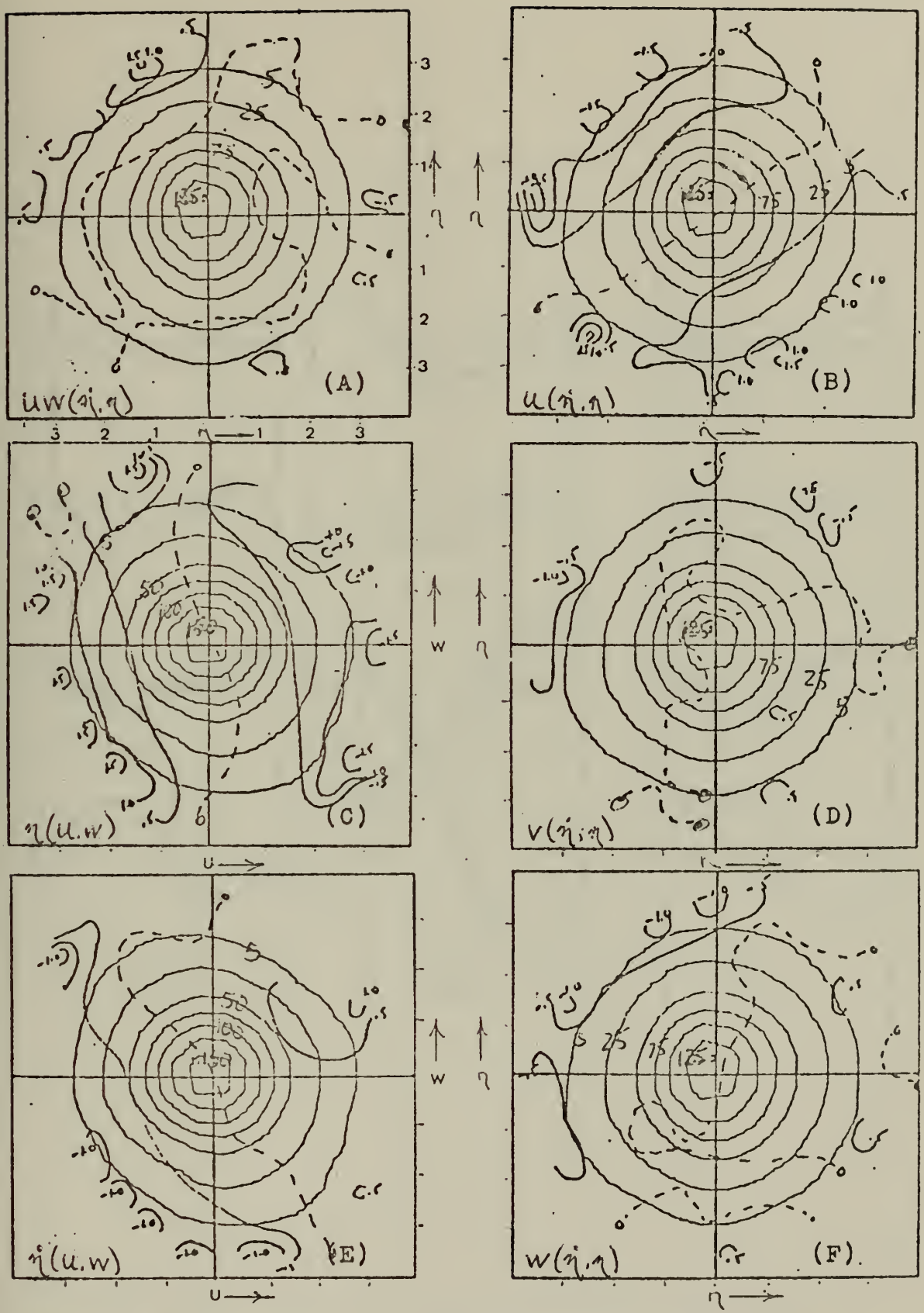

Figure 13. JPDF-CMF Patterns for Period 1, Subset 3.

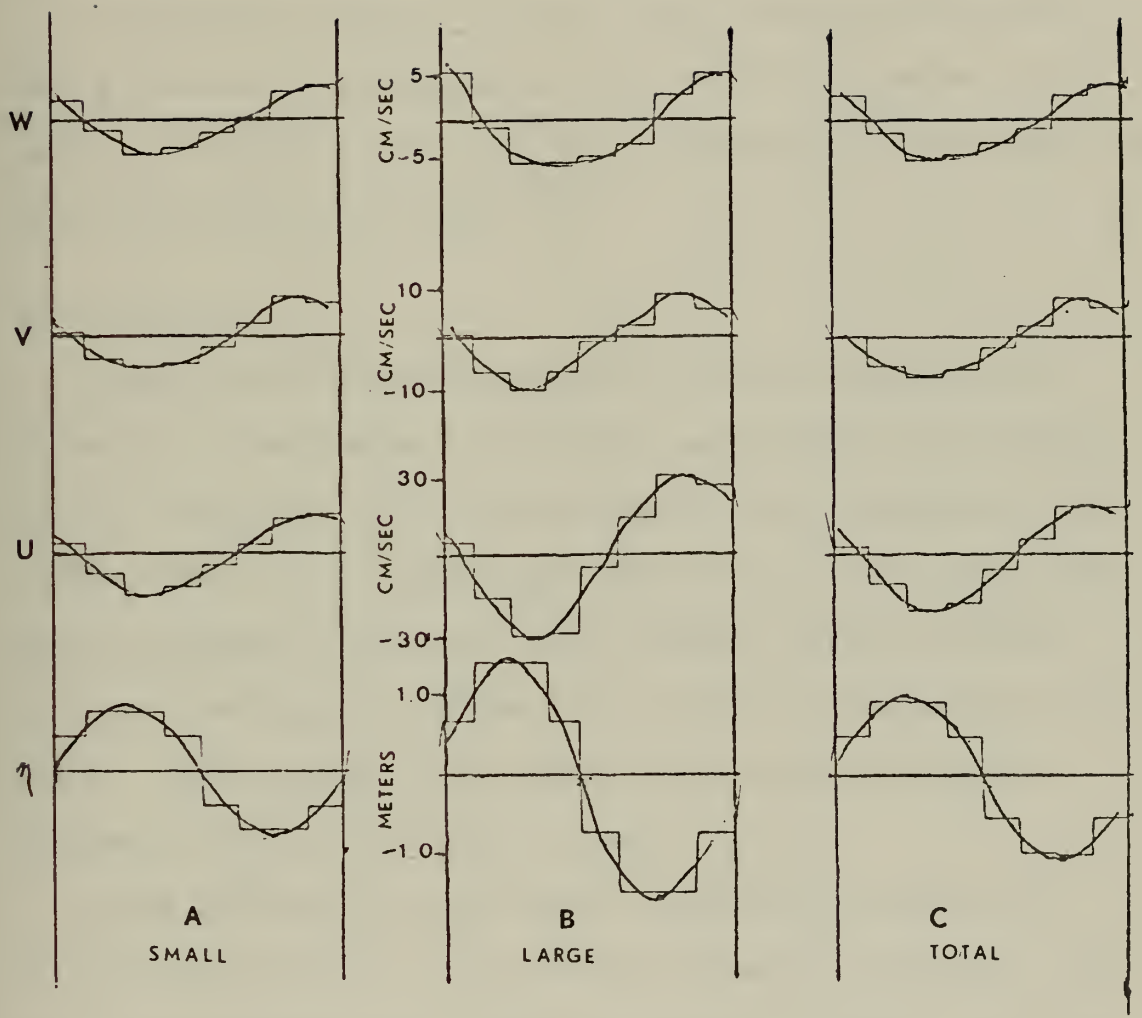

Figure 14. Phase-Amplitude Results (Components) for Period 1, Subset 2.

The relations just described can be compared to those occurring later in the period by comparing the results in Figure 14 to those in Figure 15. Results in Figure 15 correspond to a time interval which was 42 minutes after the interval corresponding to the results in Figure 14.

Considering Figure 15, the phase difference between u and w gradually increased as the period progressed until a shift of nearly 45 degrees was reached during the last subset of the period, Figure 15.

B. PERIOD 2

Significant features observed in this period were: evidence of mechanical turbulence associated with hydrostatic stability, apparent potential flow conditions and variations in the magnitude and direction of the wave-induced momentum transfer. Also changes appear to have occurred during the period in the physical make-up of the wave. This period, unlike any other period, had near potential flow conditions in both u and w.

With respect to the role of mechanical turbulence, in Figure 16 (Panel C) $\eta(u,w)$ JPDF patterns are highly elliptic with asymmetrical rings orientated so that the major axis is 135 degrees from the positive u-axis. The highly elliptic pattern will not be observed in any of the other periods. Again the turbulence is interpreted to be mechanical as in period 1 on the basis of the shift of the JPDF pattern. The corresponding cospectra in Figure 17 show only slight enhanced momentum transfer.

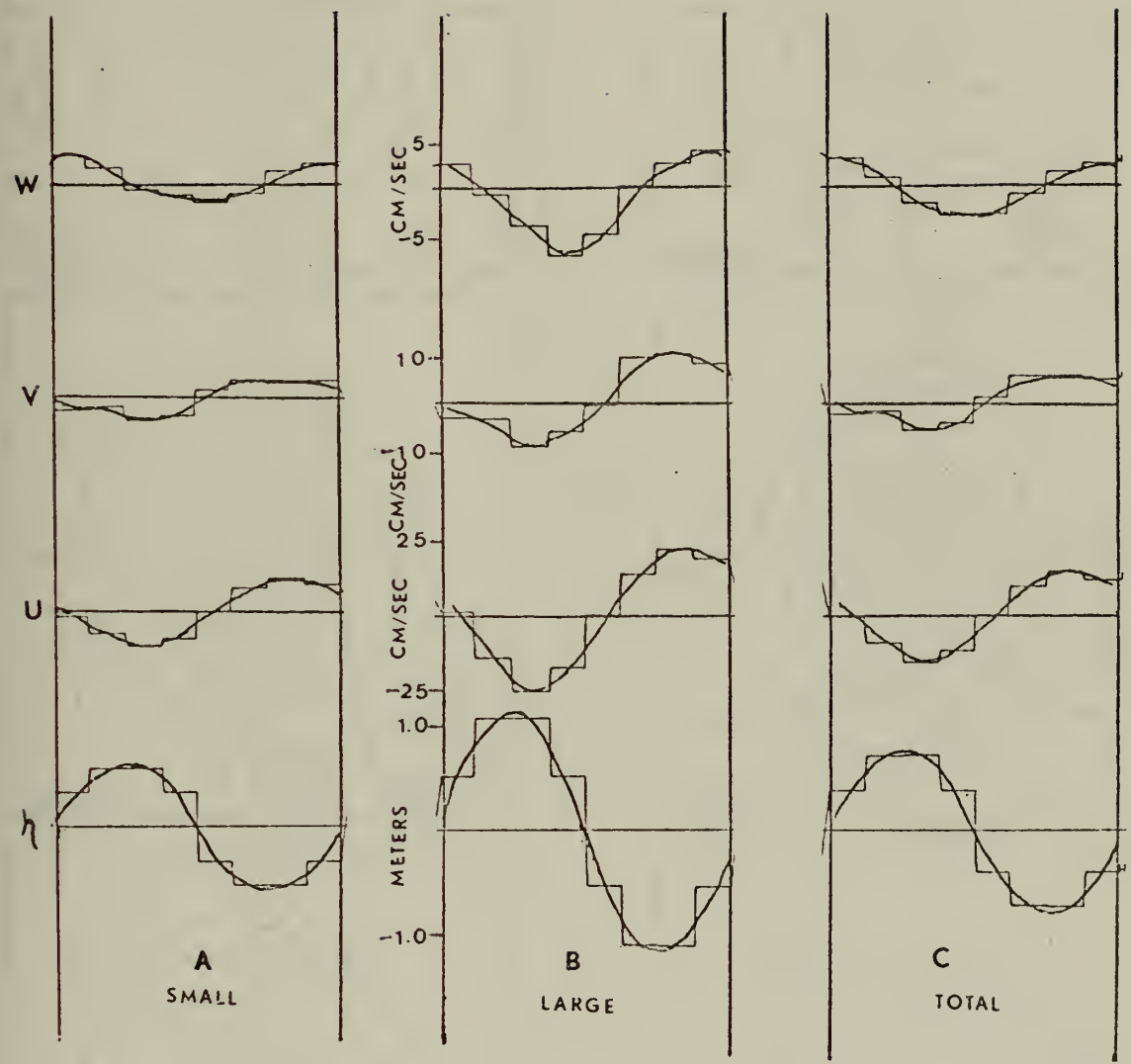

Figure 15. Phase-Amplitude Results (Components) for Period 1, Subset 4.

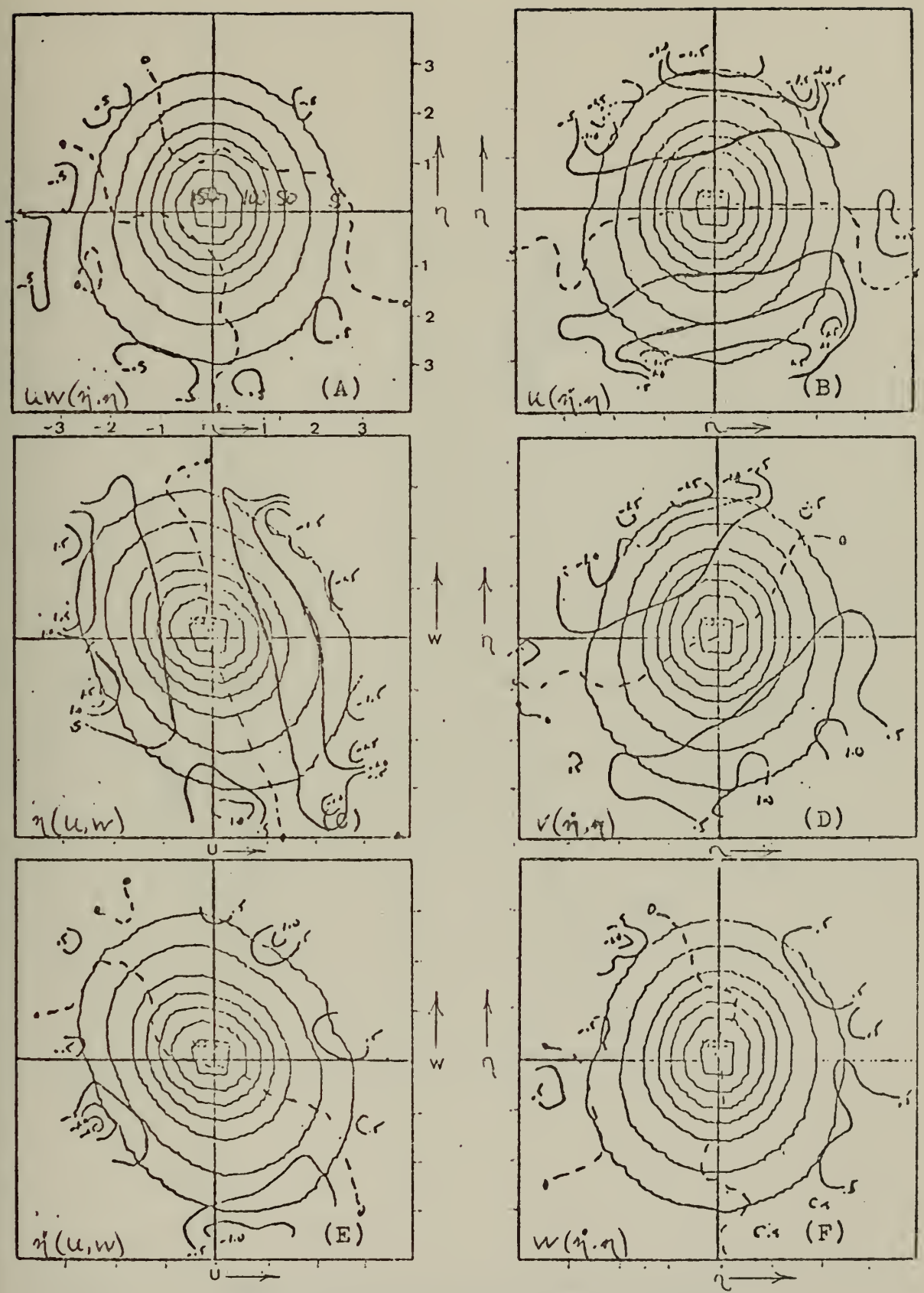

Figure 16. JPDF-CMF Patterns for Period 2, Subset 4.

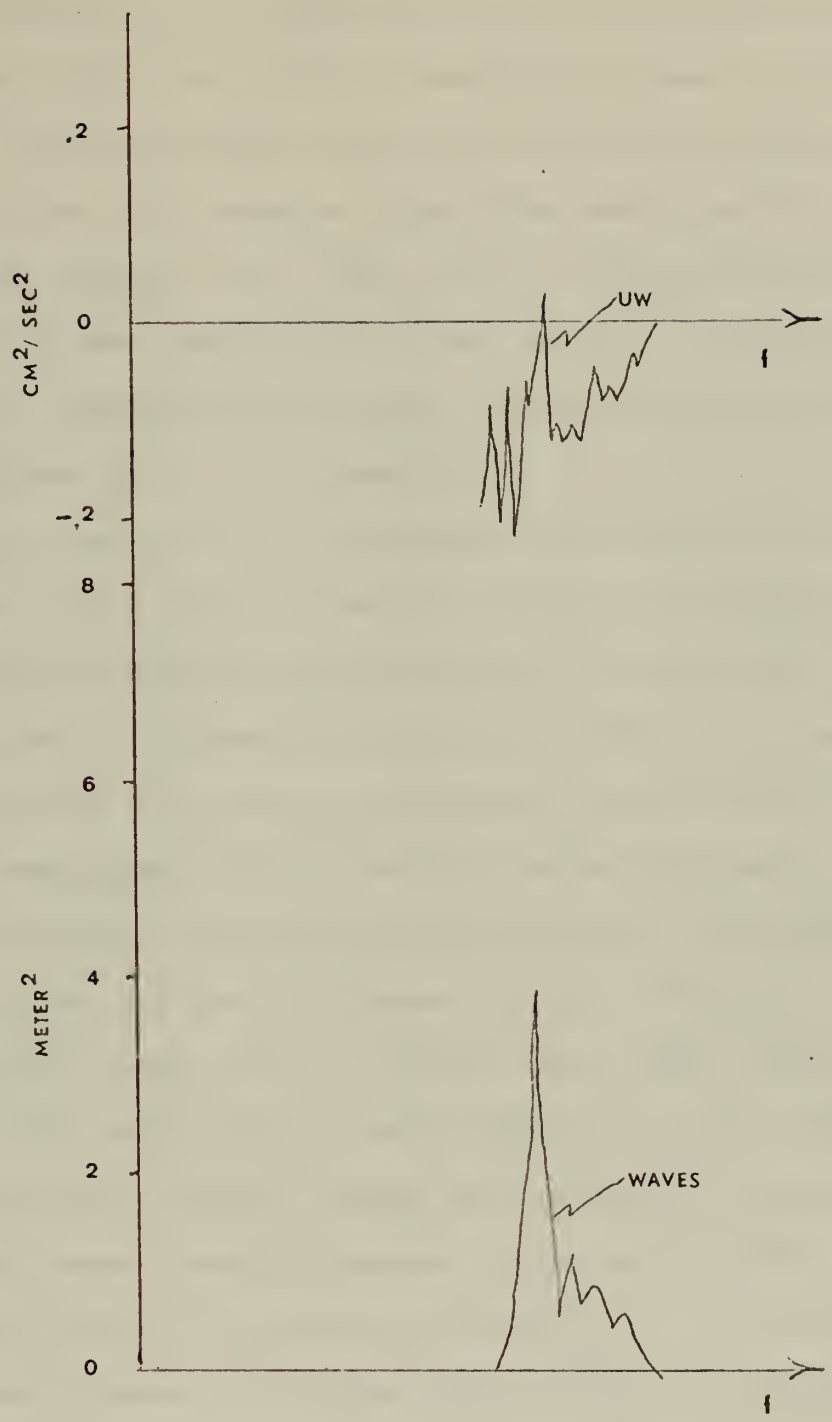

Figure 17. Spectral Results (Period 2) Including Covariance Spectra and Wave Spectra.

With respect to similarities with potential flow predictions, $u(\dot{\eta},\eta)$ and $w(\dot{\eta},\eta)$ results in Figure 16 (Panels B and F) and throughout the period reveal no significant shift of the CMF patterns from those predicted for potential flow (Figure 10). Also, $w(\dot{\eta},\eta)$ CMF patterns are weakly defined when compared to other periods. This indicated a smaller probability of joint occurrences in average fluctuations of w with $\dot{\eta}$ and η.

With respect to the suggested possibility of a different wave shape, JPDF patterns in Figure 16 (Panels B, D, and F) have a marked difference from those in any other period, such as those in Figure 11. Where previous and later periods have nearly concentric patterns showing only slight deviations from those of a sinusoidal wave, this period has more elliptical patterns with a slightly increased gradient over the wave crests. The corresponding 'statistical eddy period' is also much lower during this period than the other periods (Table I). This could be indicative of a marked change in the physical make-up of the wave, waves having sharper crests and broader troughs.

With respect to momentum transfer, uw, in relation to amplitude classes, the large wave results in Figures 18, 19, 20, and 21 appear to shift from an upward transfer of deficit momentum to a downward transfer of deficit momentum as the period progresses. To a lesser degree, the shift is also present in the total wave. This is interesting in view of the results in Figure 4 which show the general wind

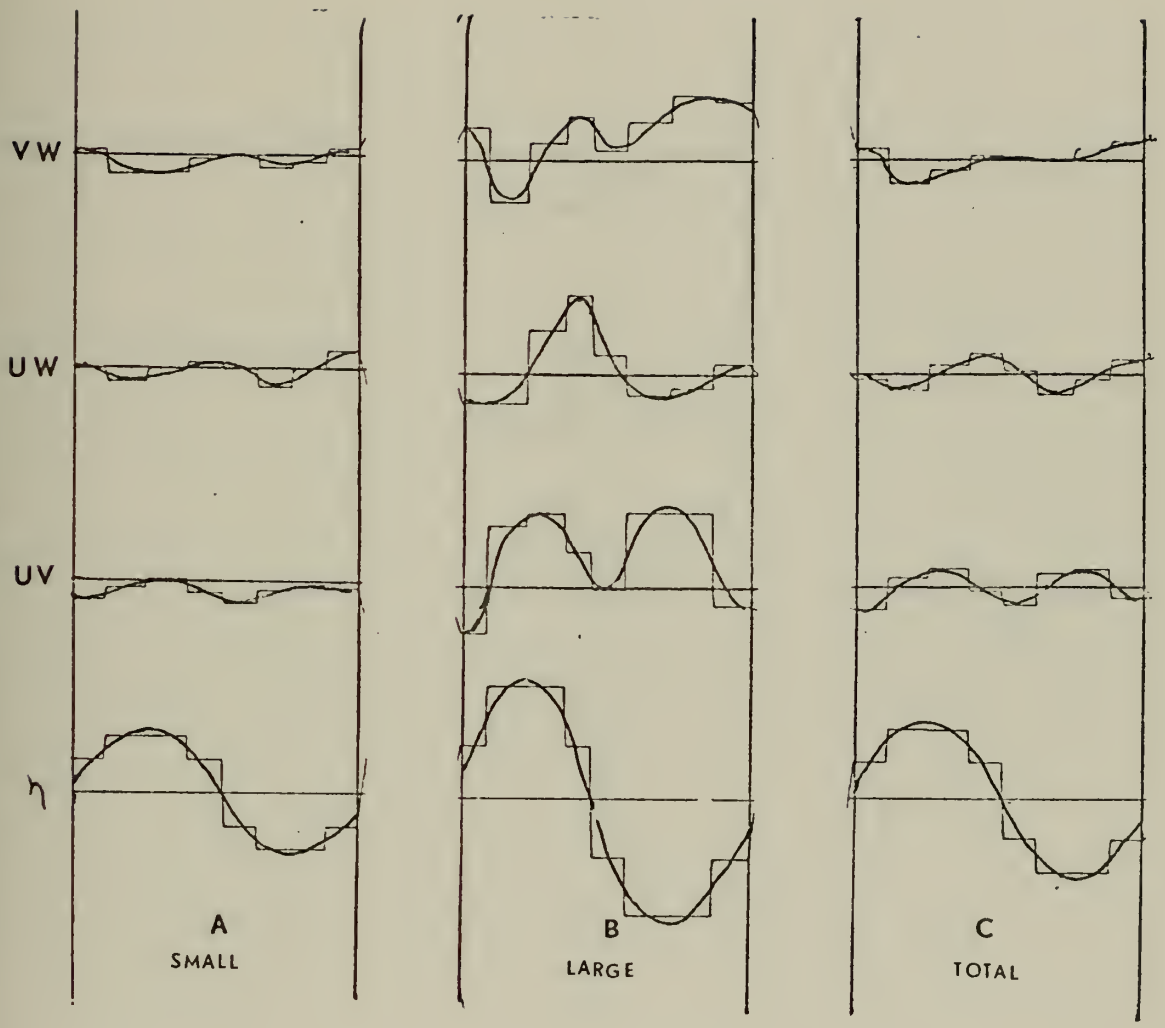

Figure 18. Phase-Amplitude Results (Stresses) for Period 2, Subset 1.

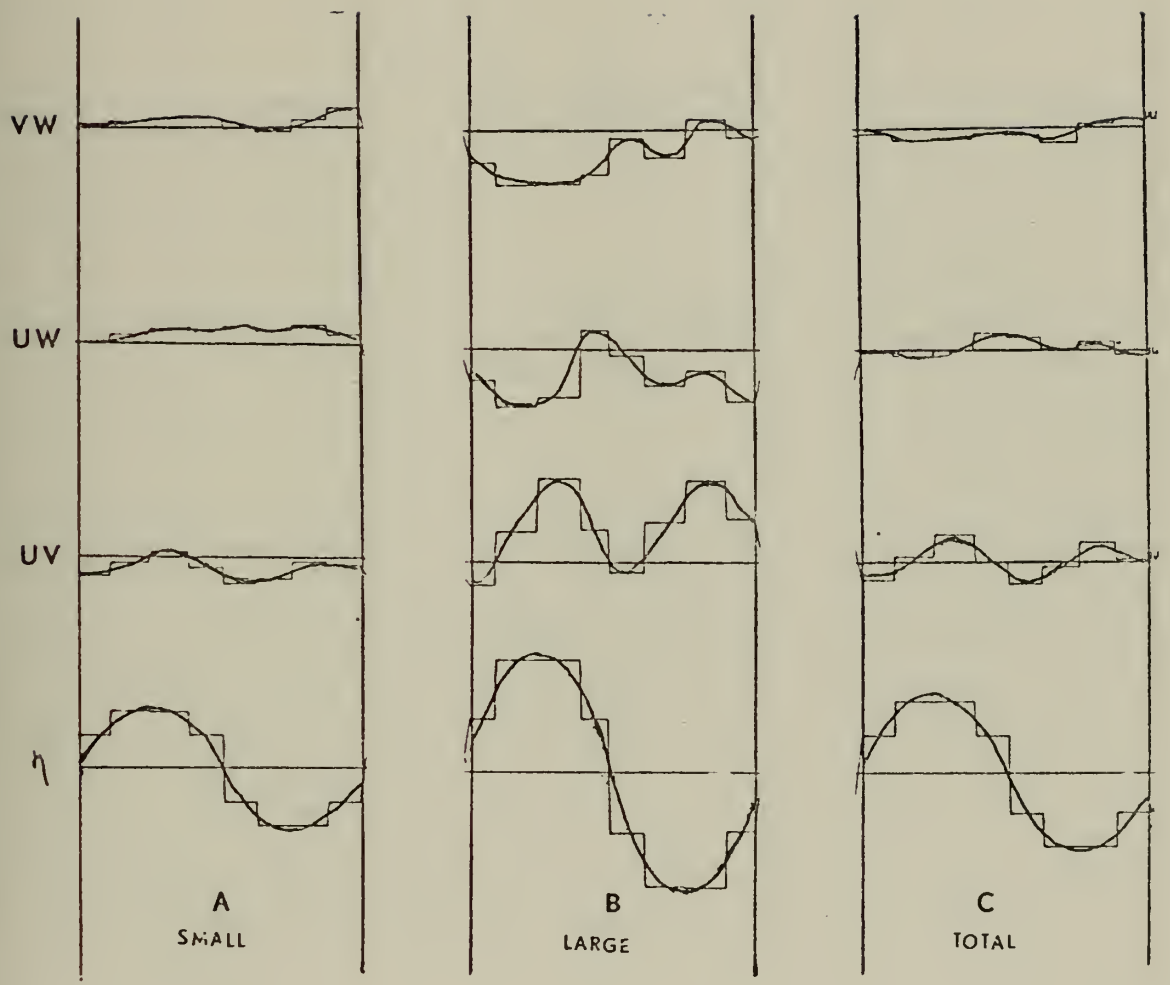

Figure 19. Phase-Amplitude Results (Stresses) for Period 2, Subset 2.

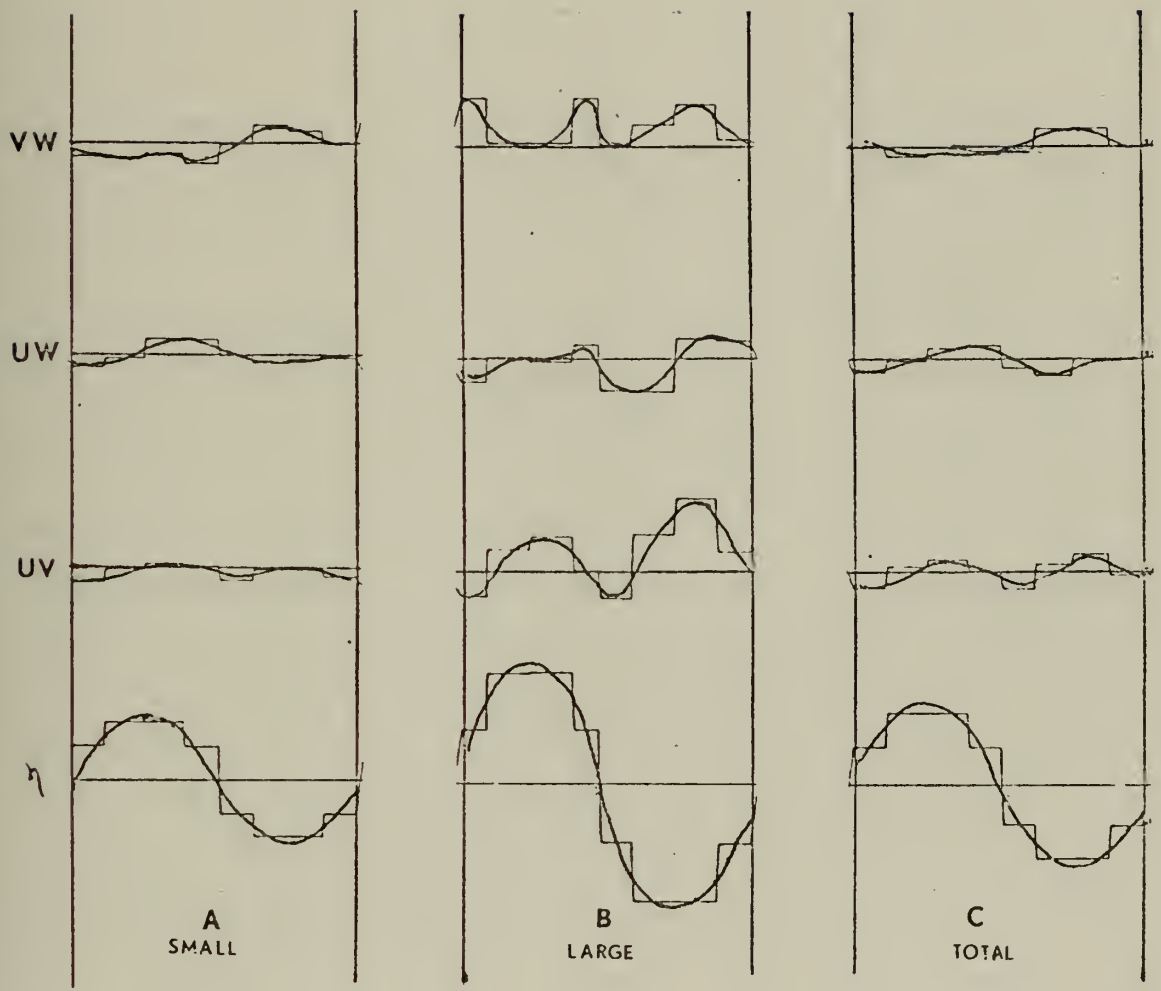

Figure 20. Phase-Amplitude Results (Stresses) for Period 2, Subset 3.

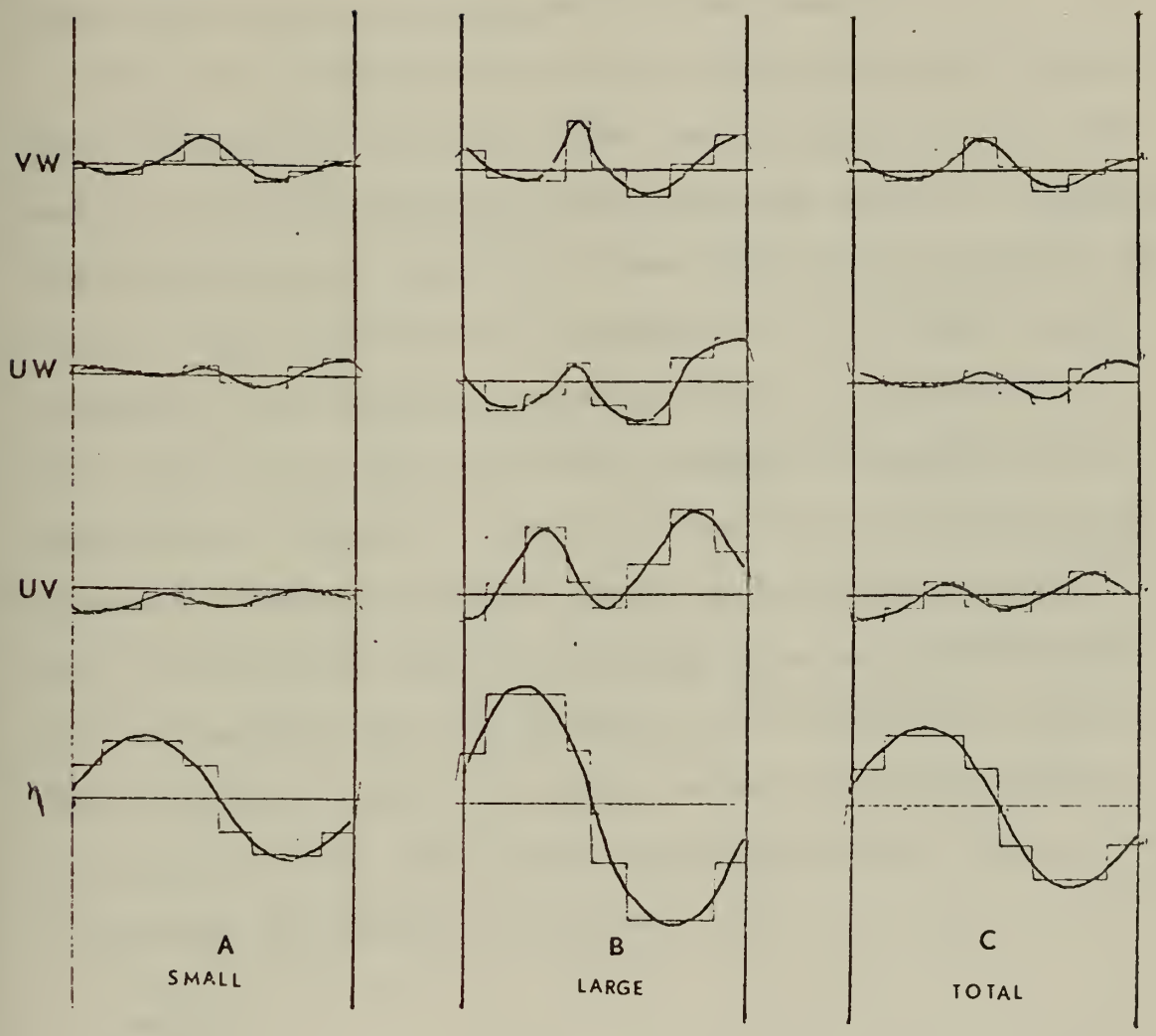

Figure 21. Phase-Amplitude Results (Stresses) for Period 2, Subset 4.

conditions for all periods. The wind has been increasing with a large increase during the last part of this period. This can possibly be attributed to what Yefimov (1970) called the complex phase as the wind speed approaches the phase speed of the predominant surface wave.

The last feature noted for this period is that the wave-form of the wave related stress (uw), Figures 18, 19, 20 and 21, also varies considerably over the period. Considering the large wave amplitude class, early in the period the largest amplitude exists in quadrant II but as the period progresses, the dominent quadrant shifts to quadrant I. With respect to the total waves, however, initially the wave-form is similar to the potential flow prediction but quadrant II becomesdominant later in the period. With respect to the third subset, the large wave amplitude class has the maximum value in quadrant III as does the total wave amplitude class. The final minutes of this period continue with the same relation found in subset three, that of maximum amplitudes in quadrant III.

C. PERIOD 3

This period differed from the other periods in that measurements were made at 3 meters. Significant features in period 3 appear to be reduction in excess momentum transfer at the frequency of the wave spectrum peak, distinct deviations from potential flow in the phase of w, and uw phase-amplitudes which differ significantly from potential flow theory.

With respect to momentum transfer, JPDF patterns in Figure 22, (Panel C) have the appearance of concentric circles. They do have a slight asymmetry in quadrant IV, representing some downward transfer of excess momentum. Spectral results for this period appear in Figure 23. The uw cospectral results reflect excess momentum transfer at the frequency of the wave spectrum peak. Such a spectral result does not agree with the JPDF axis rotation in Panel C, which is approximately 315 degrees counterclockwise from the positive u-axis.

The CMF patterns are now examined in order to determine the role of the waves in producing the (u,w) JPDF patterns in Figures 22 and 24 (Panel C). For potential flow the CMF patterns for the waves would have maximum positive values associated with negative u and zero w (Figure 10, Panel C). Maximum negative CMF values would be associated with positive u and zero w. A distinct deviation from the pattern is the clockwise rotation of both maxima and minima in the CMF patterns of approximately 35 degrees in Figures 22 and 24 (Panel C).

With respect to phase relationships, the significance of the phase shift in both extrema can be evaluated further by examining the JPDF-CMF patterns for $u(\dot{\eta},\eta)$ and $w(\dot{\eta},\eta)$ in Panels B and F. The CMF pattern orientation predicted by potential flow describes that for u fairly close with only a slight rotation as shown in Figure 22, Panel B. In the case of w, however, where maxima/minima extremes are

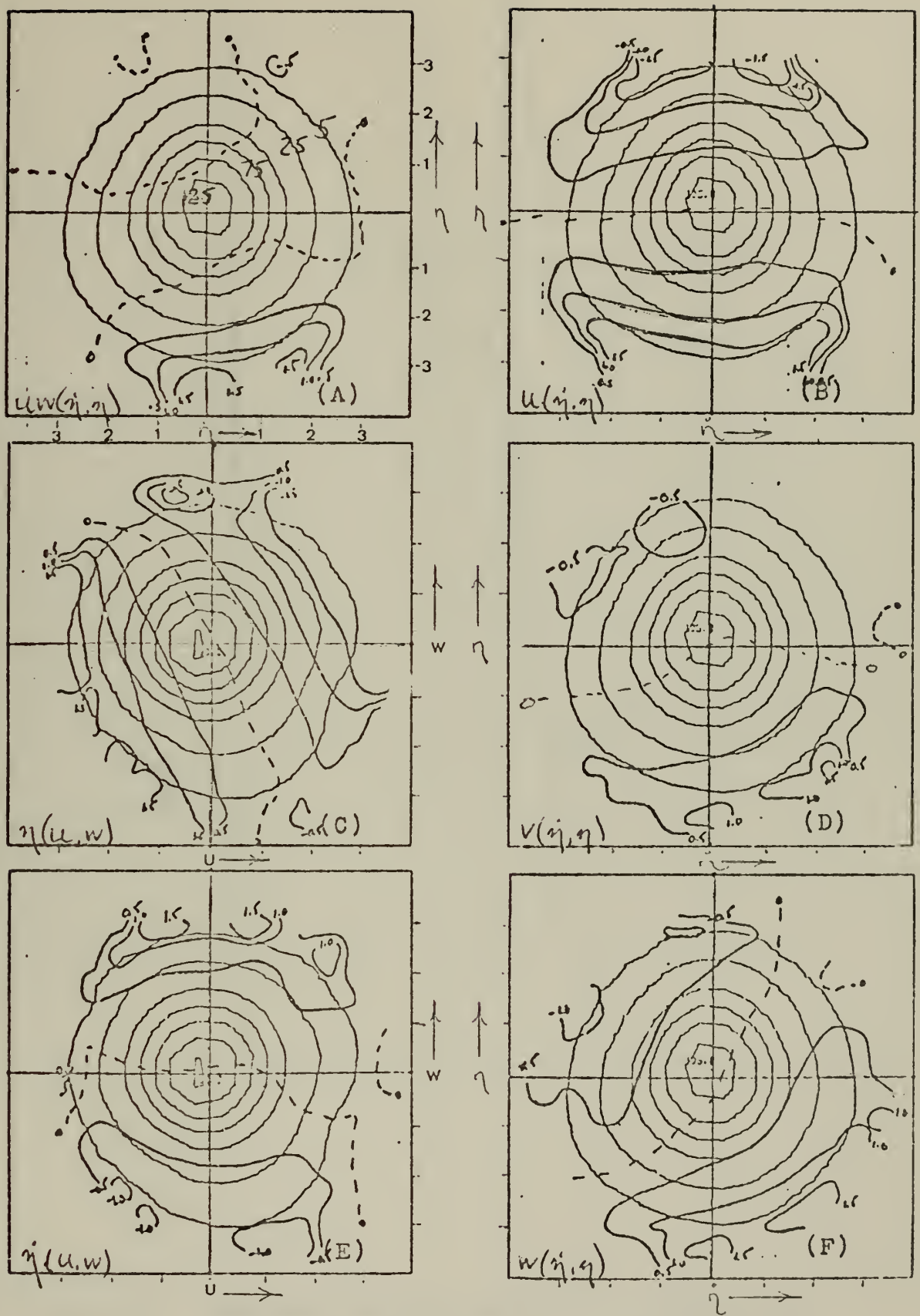

Figure 22. JPDF-CMF Patterns for Period 3, Subset 1.

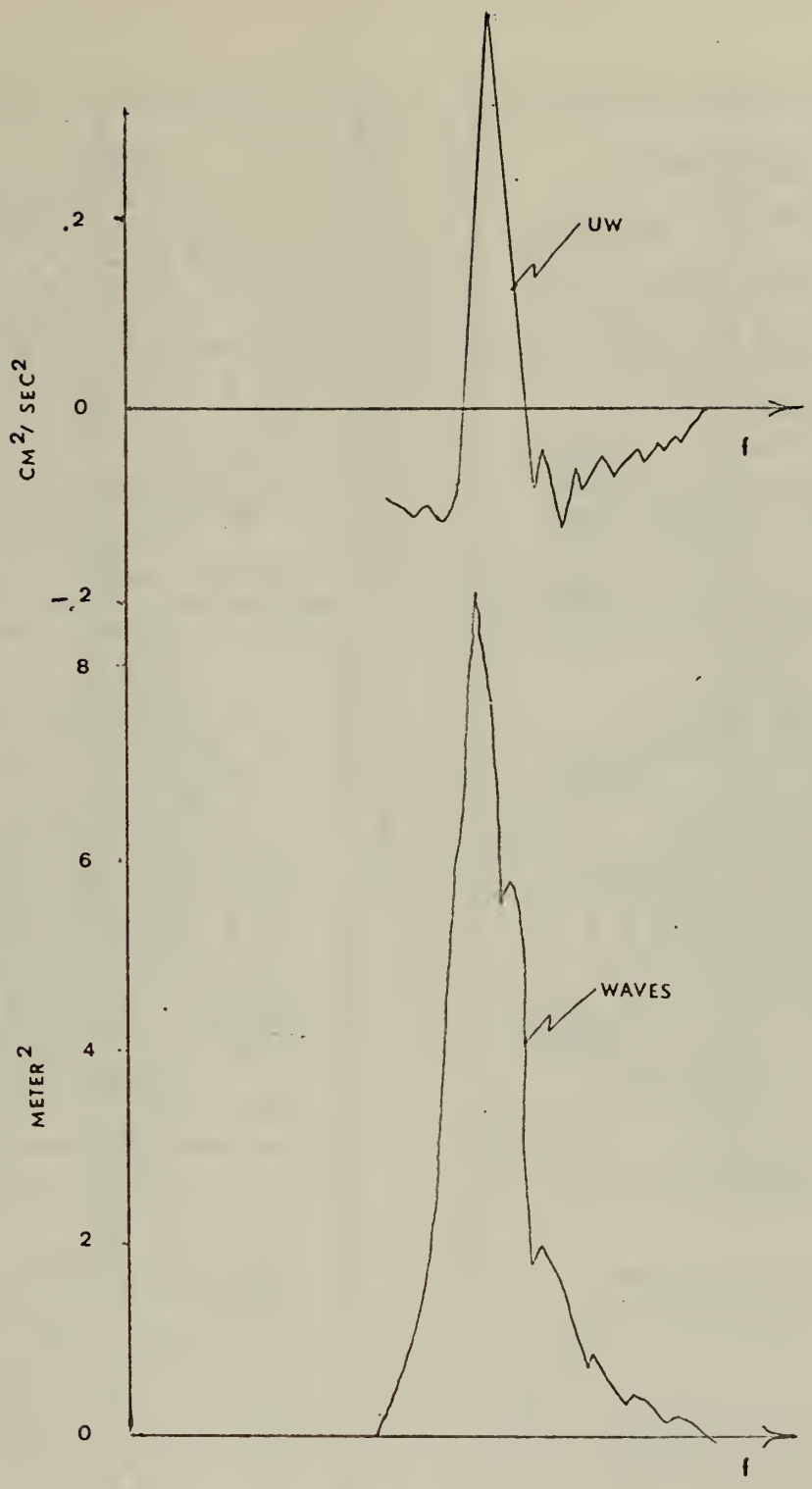

Figure 23. Spectral Results (Period 3) Including Covariance Spectra and Wave Spectra.

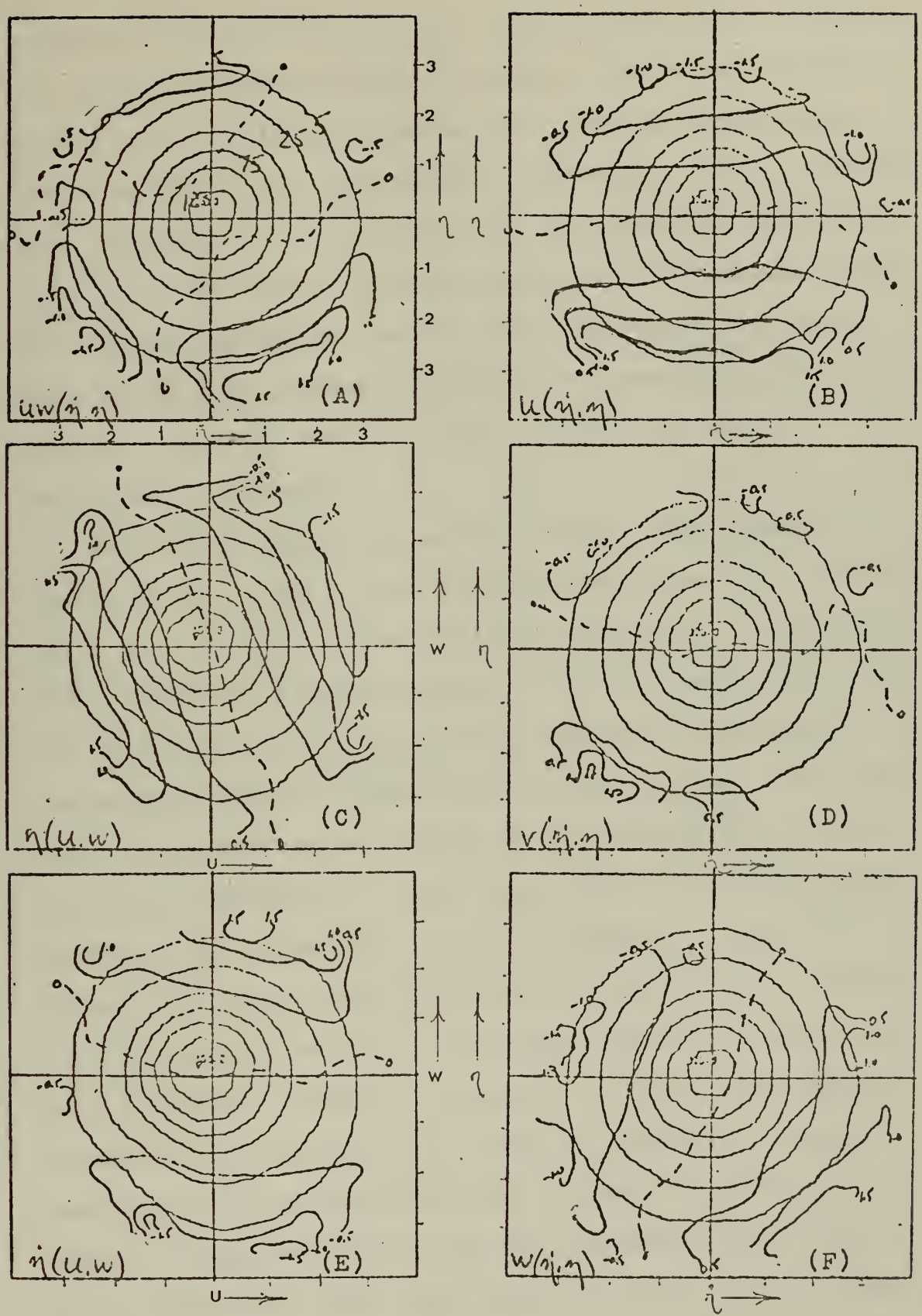

Figure 24. JPDF-CMF Patterns for Period 3, Subset 3.

supposed to be concentric around zero values of η. There is a distinct rotation backward toward positive and negative values of η. This also can be seen from the summarized phase-amplitude for this period, Figure 25. For all amplitude classes, u is also comparable to potential flow, but w is not. The latter is made evident by the minimum value of w occurring before the inflection point on the wave. This represents, perhaps, evidence of downward transfer of excess momentum over the phase of the wave due to mechanical turbulence.

To further emphasize the distortions that appear in Figure 25 for u and w, the uw phase-amplitude results and uw($\dot{\eta}$, η) JPDF-CMF results will be considered. In potential flow, Figure 4, maximum values of uw occur behind the crest and following the trough, whereas minimum values occur immediately preceding the crest and the trough. The phase relations appearing in Figure 26 are comparable to those predicted; however, the amplitudes vary over the different phases of the wave. For example, quadrant IV amplitude values are greater than the others. This is also apparent in the JPDF-CMF results. The latter result in some downward transfer of excess momentum. Quadrant III amplitudes are also greater than those in quadrant I which suggests that the occurrence of downward transfer of deficit momentum predominates as associated with hydrostatic stability, and, therefore, consistent results are obtained in this period.

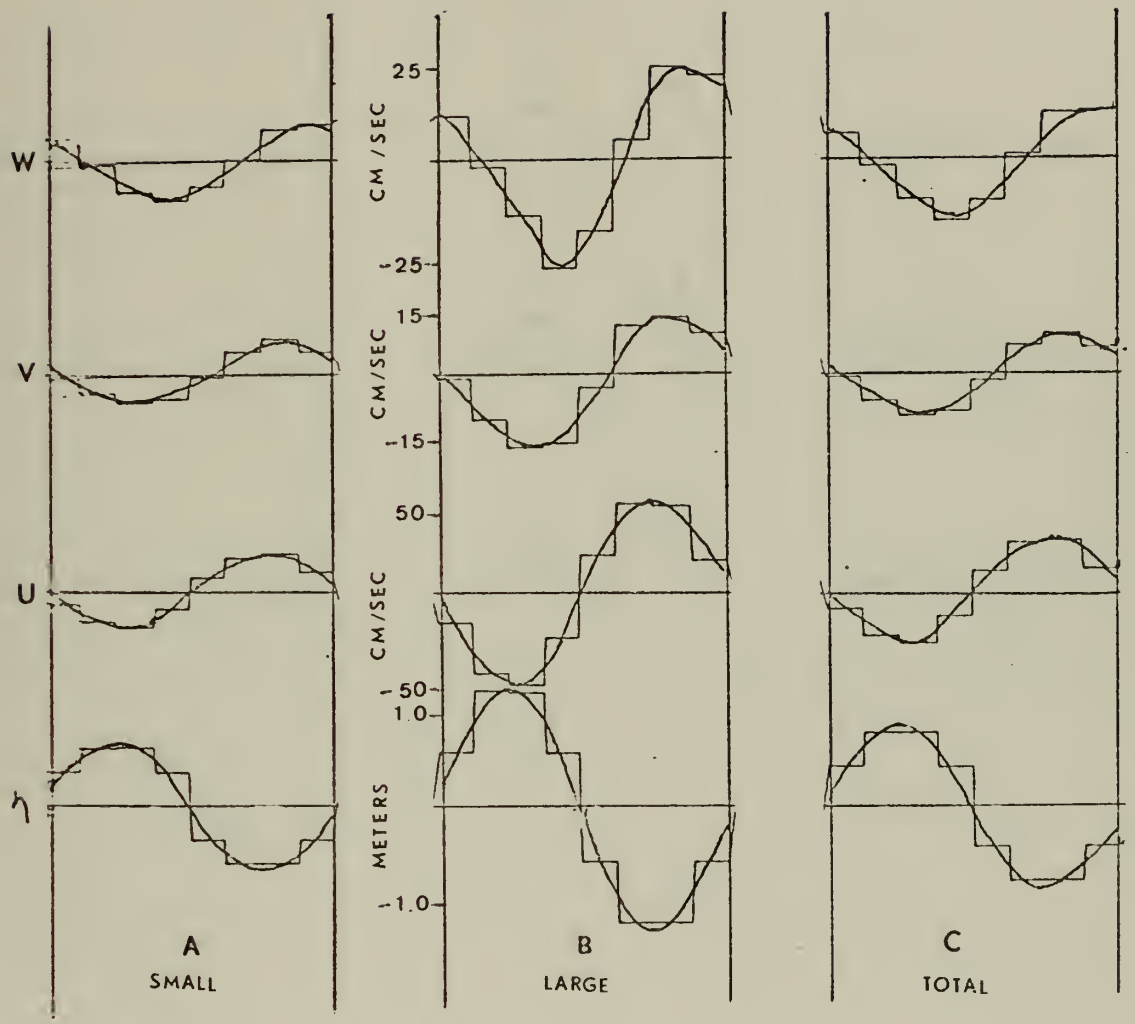

Figure 25. Phase-Amplitude Results (Components) for Period 3, Subset 2.

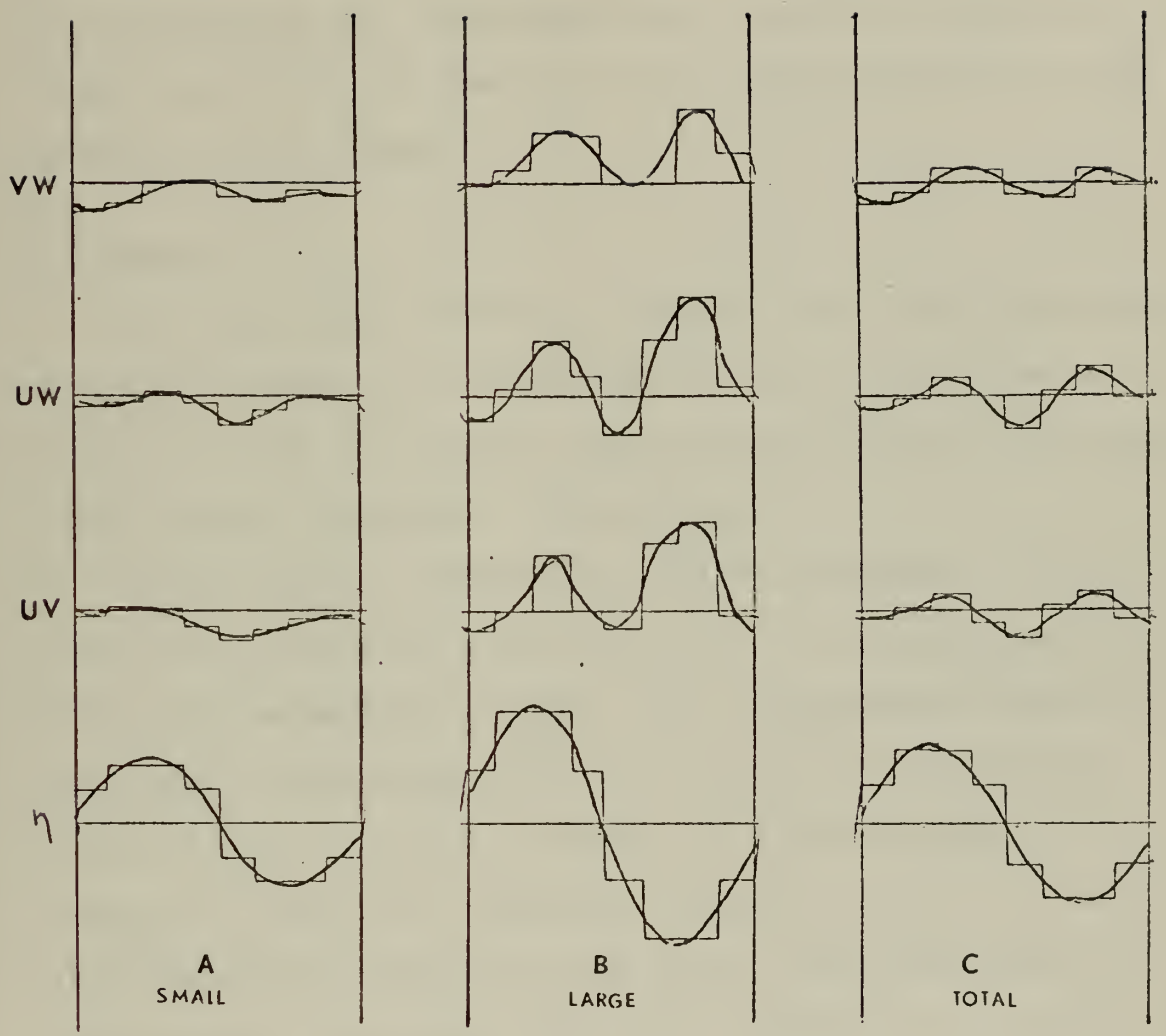

Figure 26. Phase-Amplitude Results (Stresses)for Period 3, Subset 1.

Considering the same features as above but for the JPDF-CMF uw($\dot{\eta}$, η), this period has maximum values of uw, Figure 22, (Panel A), occurring in quadrant IV but rotated slightly towards the trough position. This rotation, although not as apparent in the phase-amplitude results in Figure 26, is then consistent with the previously noted departures from potential flow theory.

D. PERIOD 4

The significant features noted in this last period are a small negative u-w correlation, a shift away from near potential flow for u and w, and definite stress deviations which suggsst wind-wave interactions.

With respect to momentum transfer processes, η(u,w) patterns in Figures 27 and 28, (Panel C), appear as minor elliptic, asymmetric circles. This appearance signifies a smaller probability of joint occurrences of negative correlation of u and w. However, the inner rings in Figure 27 (Panel C), represent a slight elliptic pattern in the opposite direction and reveal a definite positive correlation. Similarly, the phase relations of u and w in Figure 29 show u and w to be nearly in-phase. In subset 3 of this period, Figure 28, (Panel C), the positive correlation is not as evident suggesting a shift between u and w phases which can be verified by the phase-amplitude results in Figure 30.

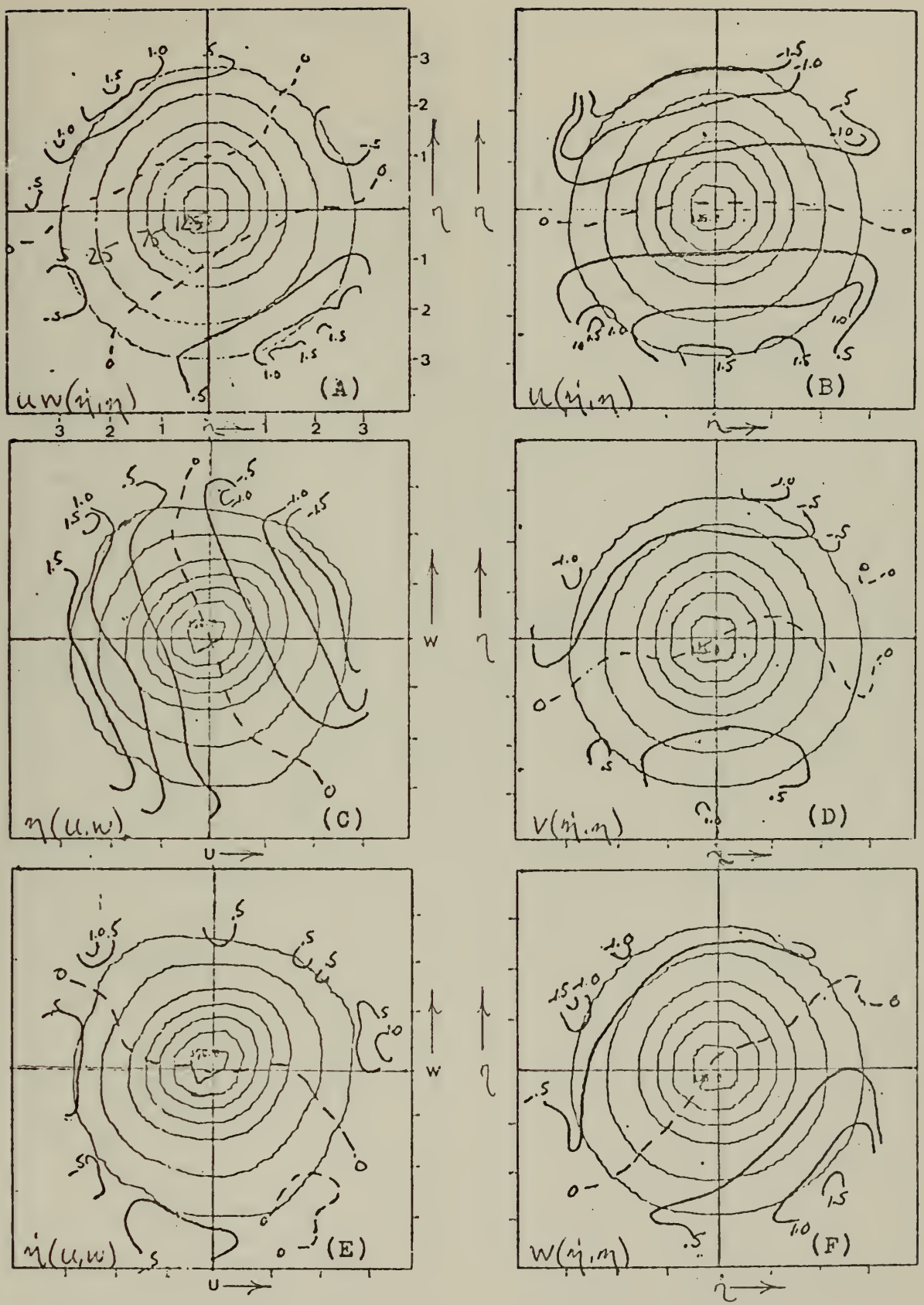

Figure 27. JPDF-CMF Patterns for Period 4, Subset 1.

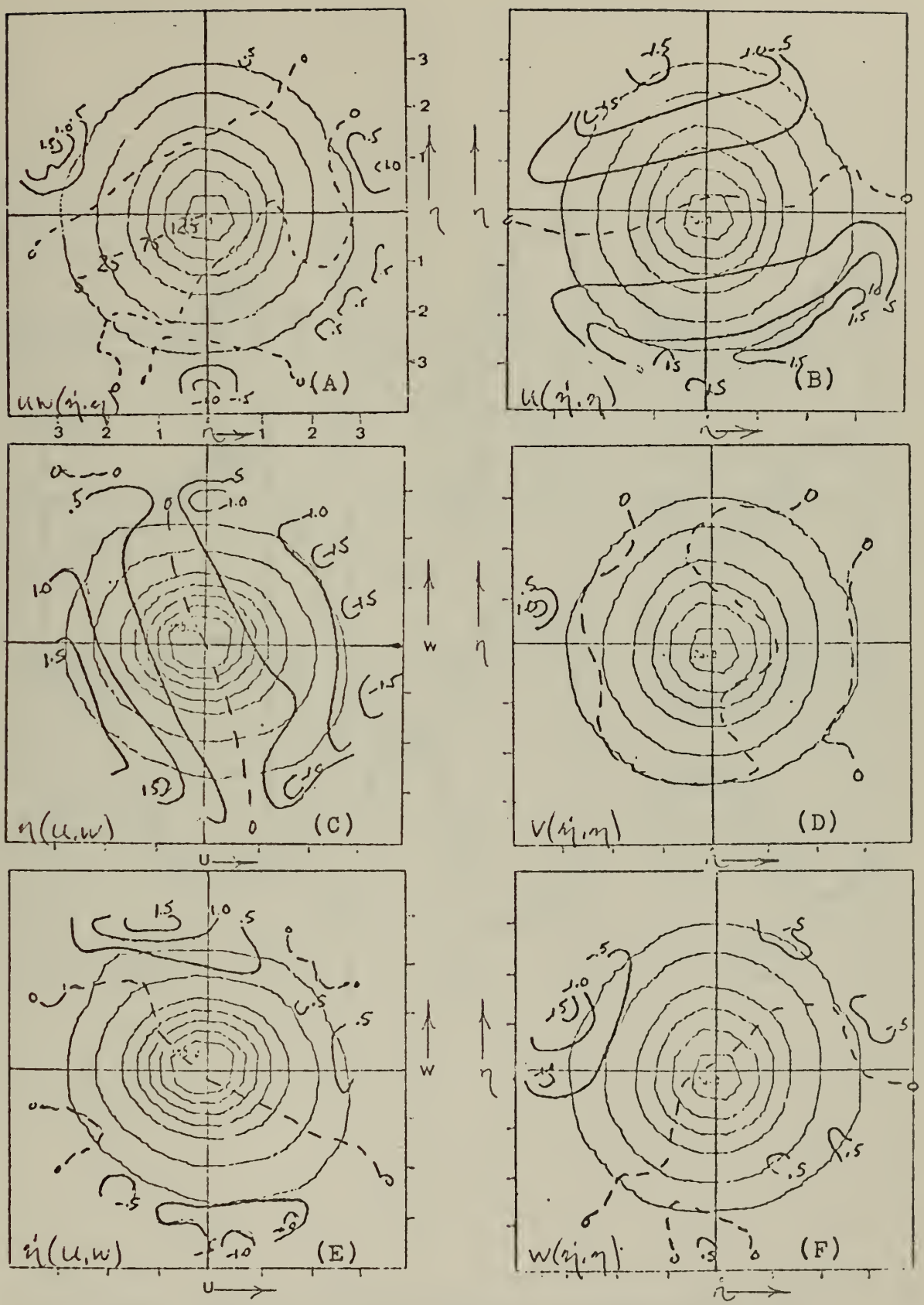

Figure 28. JPDF-CMF Patterns for Period 4, Subset 3.

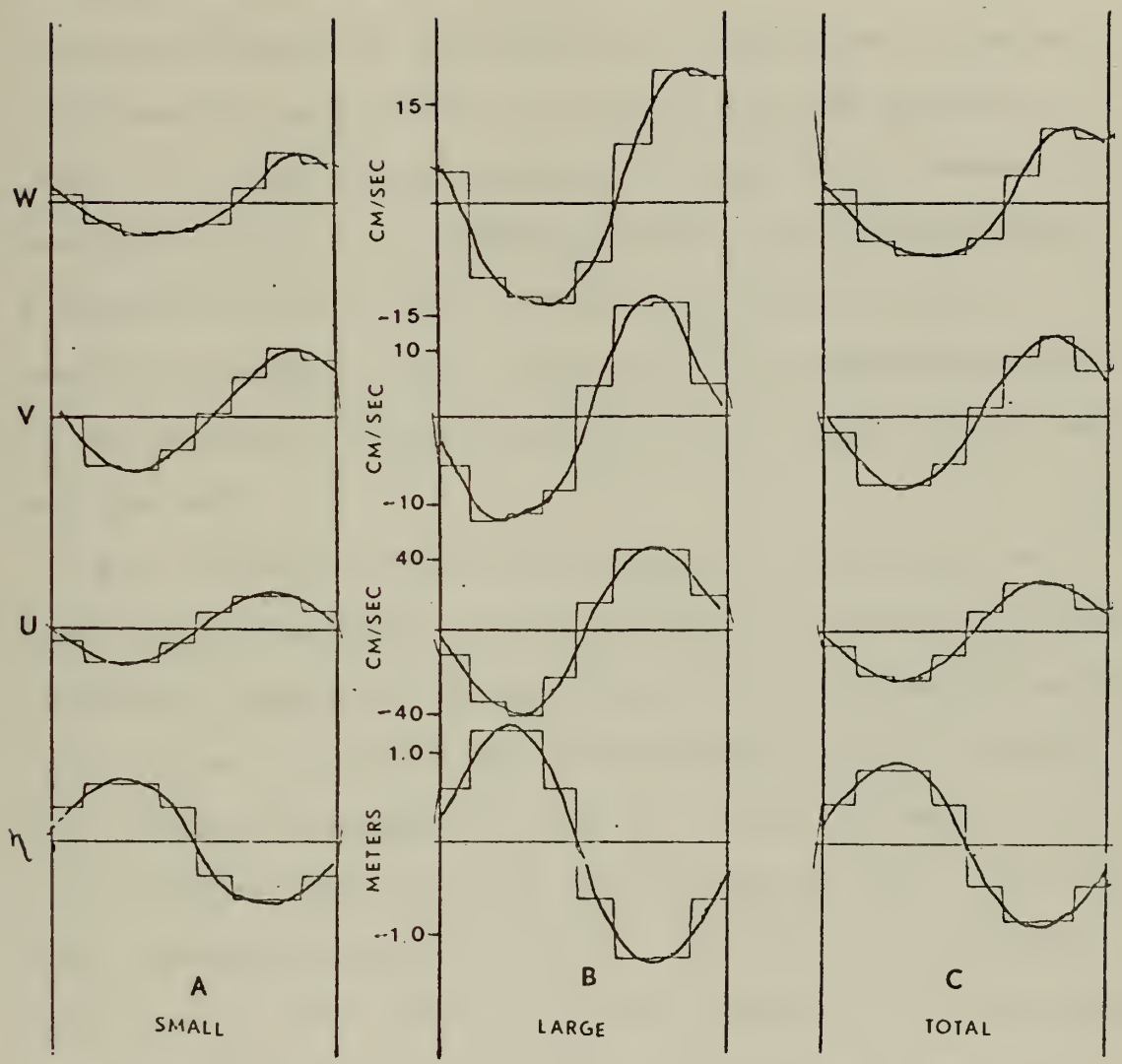

Figure 29. Phase-Amplitude Results (Components) for Period 4, Subset 1.

The orientation of CMF patterns in Figures 27 and 28, (Panel B), corresponding to $u(\dot{\eta}, \eta)$ are similar to those for near potential flow during the beginning of the period, then gradually rotate as the period progresses to a final rotation of about 30 degrees behind the crest. Similar rotations are not evident in the $w(\dot{\eta}, \eta)$ CMF patterns, (Panel F). Phase relationships in Figure 29, however, show maximum values of w occurring forward of the front node, a feature noted by Karaki (1968) and Stewart (1970). A possible reason for this rotation of the CMF pattern may be the turbulent interaction between the near surface wind and the wave.

With respect to phase variations of the stress uw, initially the maximum positive values of uw, Figure 31 are forward of quadrants II and IV and are not equal in magnitude. Later in Figure 33, the magnitude of uw is nearly equal in both quadrants II and IV. In both cases, however, a sufficient shift is noted from potential flow. This was also observed by Kendall (1970). The $uw(\dot{\eta}, \eta)$ patterns, Figures 27 and 28, (Panel A), also reflects these deviations from potential flow since higher CMF values appear in quadrants II and IV. However, looking at the phase relationships in Figure 31, quadrant IV, downward transfer of excess momentum is the largest for both large and total waves. During the middle of the period, Figure 32, quadrant II is predominant over large waves, while quadrant IV is the dominant over total waves. During the last part of

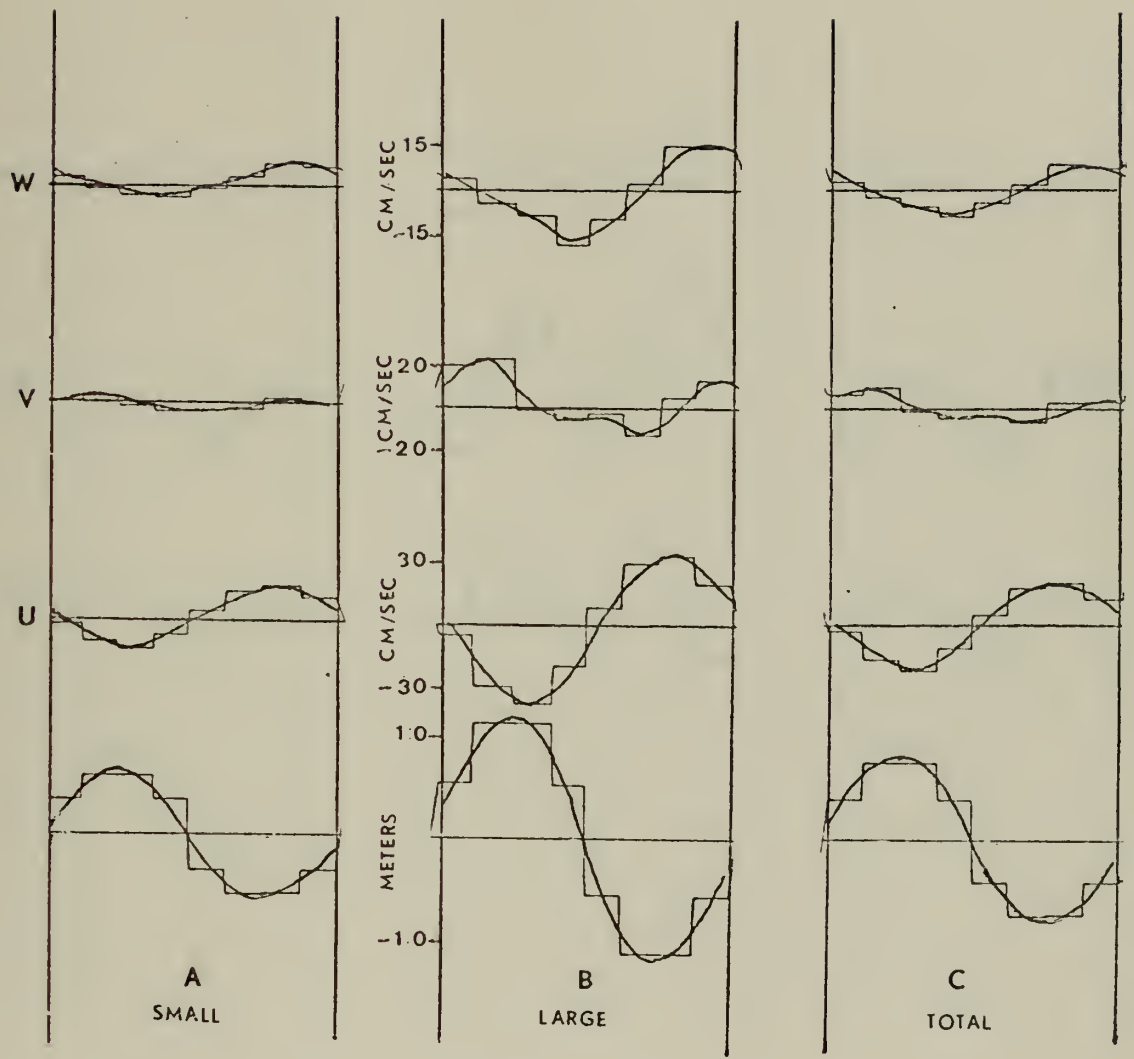

Figure 30. Phase-Amplitude Results (Components) for Period 4, Subset 3.

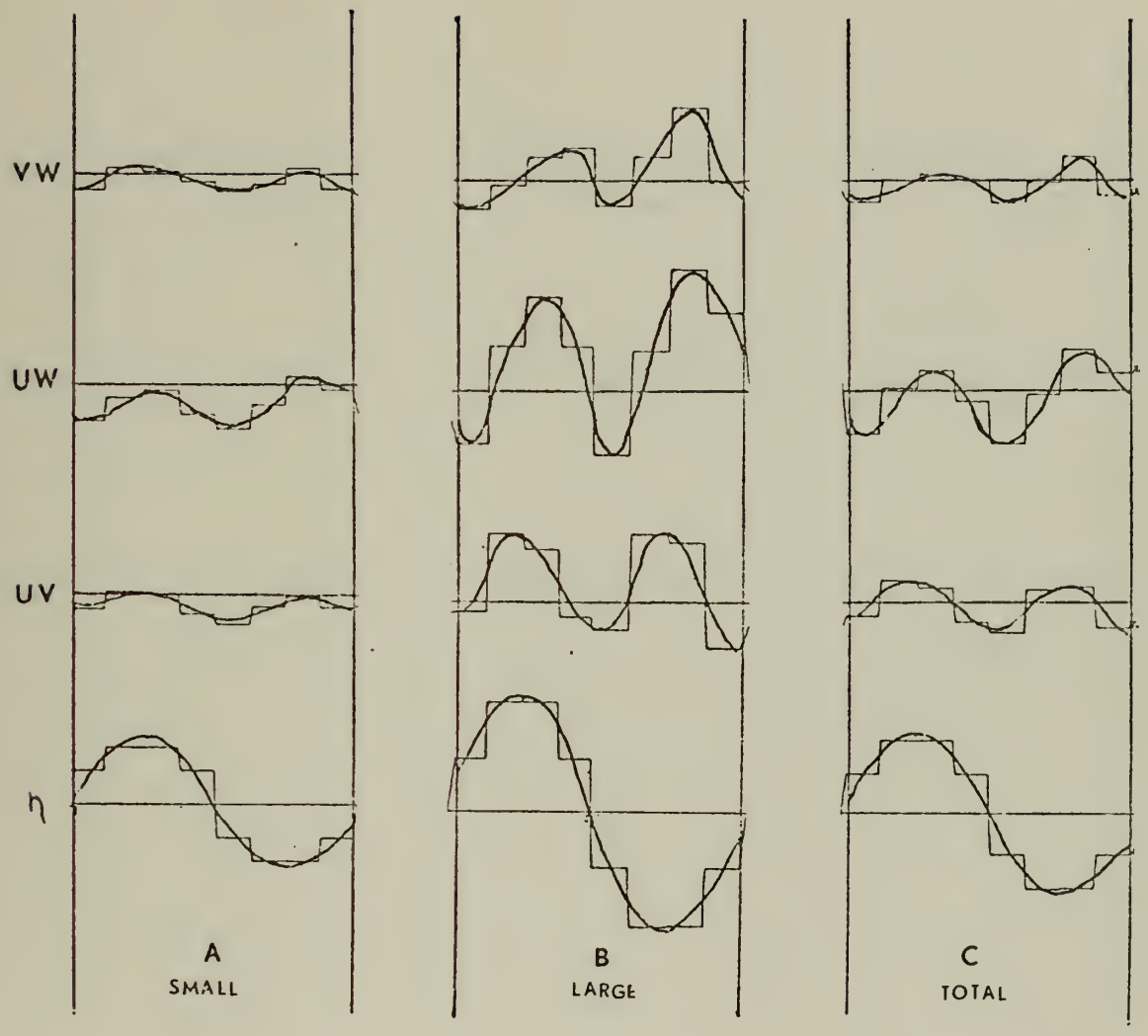

Figure 31. Phase-Amplitude Results (Stresses) for Period 4, Subset 1.

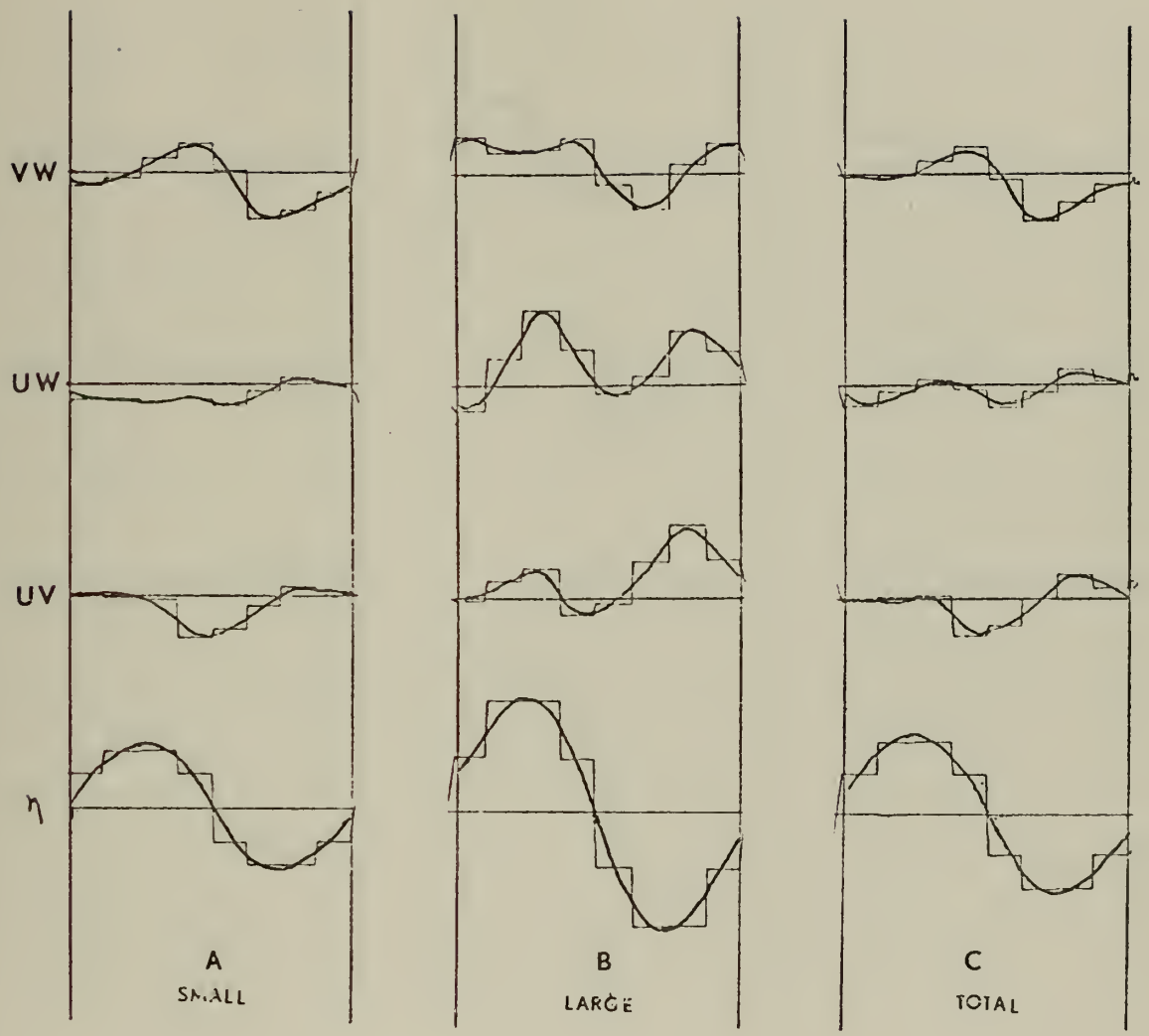

Figure 32. Phase-Amplitude Results (Stresses) for Period 4, Subset 2.

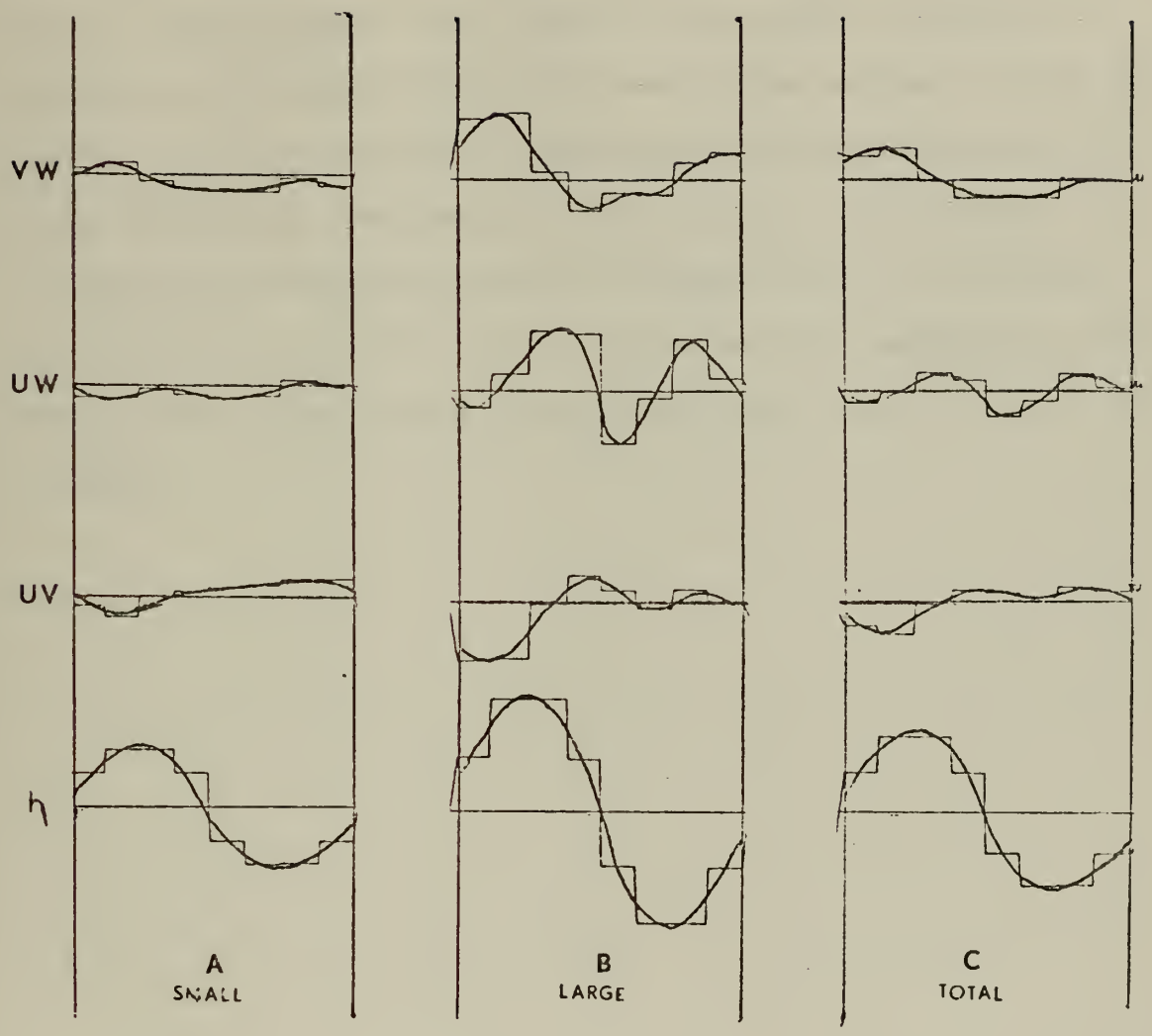

Figure 33. Phase-Amplitude Results (Stresses) for Period 4, Subset 3.

the period, Figure 33, large uw stress amplitudes appear in quadrant II for both large and total waves. In general, there is a shift from an initial downward transfer of excess momentum to an upward transfer of deficit momentum. This suggests that, due to the waves' influence, momentum is being transfered towards the surface during the first half of the period and transfered away from the surface during the last half of the period. During the reversal of momentum transfer between the first part of the period to the last part of the period, mechanical turbulence may well be the important factor in the momentum transfer.

V. SUMMARY AND CONCLUSIONS

Analyses were performed on observational data obtained over ocean waves. These analyses provided results on the phase and amplitude relationship of the wave-induced fluctuations. These results were interpreted with respect to potential flow predictions for a wave propagating beneath a shear flow and the role of turbulence in wind-wave coupling.

A significant feature was the consistent rotation of the CMF pattern in the $u(\dot{\eta}, \eta)$ and $w(\dot{\eta}, \eta)$ results from the orientation which would correspond to potential flow. This rotation was noticeable in all periods analyzed to some degree. Also observed was the absence of the quadrature relationship of u and w as predicted by potential flow theory.

In comparison to potential flow predictions which have equal magnitudes of uw phase-amplitude in all quadrants, the uw phase-amplitude results revealed variations of magnitude over different phases of the wave. This suggests that nonlinear processes are responsible for momentum transfer in wind-wave coupling.

Therefore, wave-caused motion of the air in the near-water layer was observed to be essentially nonpotential. This was most evident in periods 1, 3, and 4 with a lesser deviation from potential flow during period 2. However, during period 2, a marked change was taking place in the physical make-up of the wave.

BIBLIOGRAPHY

1. Kinsman, B., Wind-Waves, Their Generation and Propagation on the Ocean Surface, 676 pp., Prentice-Hall, Inc., 1965.

2. Phillips, O. M., The Dynamics of the Upper Ocean, 261 pp., Cambridge Press, 1966.

3. Davidson, K. L., and Frank, A. J., "Wave-Related Fluctuations in the Airflow Above Natural Waves," Journal of Physical Oceanography, 3(1), (in press).

4. Davis, R. E., "On the Turbulent Flow over a Wavy Boundary," Journal of Fluid Mechanics, v. 42, part 4, p. 721-731, 1970.

5. Davis, R. E., "On Prediction of the Turbulent Flow over a Wavy Boundary,"Journal of Fluid Mechanics, 52, p. 721 - 732, 1972.

6. Holland, J. Z., "A Statistical Method for Analyzing Wave Shapes and Phase Relationships of Fluctuating Geophysical Variables," Journal of Physical Oceanography, 2, 1973.

7. Kendall, J. M., "The Turbulent Boundary Layer over a Wall with Progressive Surface Waves," Journal of Fluid Mechanics, 41(2), p. 259-281, 1970.

8. Kondo, J., Fujinawa, Y., and Naito, G., "Wave-Induced Wind Fluctuations over the Sea," Journal of Fluid Mechanics, v. 51, part 4, p. 751-771, 1972.

9. Manton, M. J., "On the Streamline Configuration Associated with Miles' Theory of Sea Wave Growth," Boundary-Layer Meteorology, p. 264-276, 1971.

10. Miles, J. W., "On the Generation of Surface Waves by Shear Forces," Journal of Fluid Mechanics, v. 6, part 4, p. 185-204, 1957.

11. Rudnick, P., "Motion of a Large Spar Buoy in Sea Waves," Journal of Ship Research, v. 11, No. 4, p. 257-267, 1967.

12. Stewart, R. H., "Laboratory Studies of the Velocity Field over Deep-Water Waves," Journal of Fluid Mechanics, v. 42, part 4, p. 733-754, 1970.

13. Yefimov, V. V., "On the Structure of the Wind Velocity Field in the Atmospheric Near-Water Layer and the Transfer of Wind Energy to Sea Waves," Atmospheric and Oceanic Physics, v. 6, No. 19, p. 1043-1058, translated by McIntosh, J. D. L., 1970.

14. Scripps Institute of Oceanography, San Diego, California, SIO Reference 65-12, ONR Contract Nonr 2216(05), by E. D. Bronson, and L. R. Glosten, FLIP, Floating Instrument Platform, 21 pp., 1965.

15. University of Michigan, ONR Contract No. N00014-67-A-0181-0005, An Investigation of the Influence of Water Waves on the Adjacent Airflow, by K. L. Davidson, 1970.

16. U. S. Atomic Energy Commission, Washington, D. C., TID-24585, An Application of Some Statistical Techniques to the Study of Eddy Structures, by J. Z. Holland, 378 pp., 1968.

17. Stanford University, ONR Contract No. Nonr-225(71), NR062-320, An Experimental Investigation of the Structure of a Turbulent Wind over Water Waves, by S. Karaki, and E. Y. Hsu, 1968.

18. University of Michigan, ONR Contract No. N00014-67-A-0181-0005, An Investigation of the Structure of Turbulence Fluxes of Momentum and Heat over Waves, by D. J. Portman, K. L. Davidson, and M. A. Walter, August 1970.

19. Reynolds, W. C., The Mechanics of an Organized Wave in a Turbulent Shear Flow, unpublished manuscript, Department of Mechanical Engineering, Stanford University, 39 pp., 1968.

20. Stewart, R. H., Laboratory Studies of the Velocity Field over Deep-Water Waves, Ph.D. dissertation, University of California, San Diego, California, 1969.

21. Bingham, G. S., Spectra of Turbulent Fluctuations over Ocean Waves, M.A. Thesis, Naval Postgraduate School, Monterey, California, 1972.

22. Frank, A. J., An Investigation of the Properties and Influence of Wave-Related Organized Motion in the Adjacent Airflow, M.A. Thesis, Naval Postgraduate School, Monterey, California, 1971.

INITIAL DISTRIBUTION LIST

		No. Copies
1.	Defense Documentation Center Cameron Station Alexandria, Virginia 22314	2
2.	Library, Code 0212 Naval Postgraduate School Monterey, California 93940	2
3.	Professor Kenneth L. Davidson, Code 51Ds Department of Meteorology Naval Postgraduate School Monterey, California 93940	5
4.	Lieutenant Commander Stanley P. Thompson, USN COMCARDIV FIVE/CTF77 FPO San Francisco 96601	3
5.	Professor Noel Boston, Code 58Bb Department of Oceanography Naval Postgraduate School Monterey, California 93940	1
6.	Professor Edward Thornton, Code 58Tm Department of Oceanography Naval Postgraduate School Monterey, California 93940	1
7.	Department of Meteorology Naval Postgraduate School Monterey, California 93940	2
8.	Professor G. J. Haltiner, Code 51Ha Department of Meteorology Naval Postgraduate School Monterey, California 93940	1
9.	Dr. Donald J. Portman Department of Meteorology and Oceanography University of Michigan Ann Arbor, Michigan 48103	1

10. Professor R. T. Williams, Code 51Wu — 1
Department of Meteorology
Naval Postgraduate School
Monterey, California 93940

11. Commander, Naval Weather Service Command — 1
Naval Weather Service Headquarters
Washington Navy Yard
Washington, D. C. 20390

Security Classification

DOCUMENT CONTROL DATA - R & D

(Security classification of title, body of abstract and indexing annotation must be entered when the overall report is classified)

1. ORIGINATING ACTIVITY (Corporate author)

Naval Postgraduate School
Monterey, California 93940

2a. REPORT SECURITY CLASSIFICATION

Unclassified

2b. GROUP

3. REPORT TITLE

Wave-Related Disturbances in the Velocity Field over Ocean Waves

4. DESCRIPTIVE NOTES (Type of report and inclusive dates)

Master's Thesis; September 1972

5. AUTHOR(S) (First name, middle initial, last name)

Stanley P. Thompson

6. REPORT DATE	7a. TOTAL NO. OF PAGES	7b. NO. OF REFS
September 1972	77	22

8a. CONTRACT OR GRANT NO.	9a. ORIGINATOR'S REPORT NUMBER(S)
b. PROJECT NO.	
c.	9b. OTHER REPORT NO(S) (Any other numbers that may be assigned this report)
d.	

10. DISTRIBUTION STATEMENT

Approved for public release; distribution unlimited.

11. SUPPLEMENTARY NOTES	12. SPONSORING MILITARY ACTIVITY
	Naval Postgraduate School Monterey, California 93940

13. ABSTRACT

Velocity fluctuations over ocean waves and wave heights are examined using joint probability density function-conditional mean function (JPDF-CMF) analyses. Results are compared with theoretical predictions from wind-wave coupling models which provide for interaction between the wave-induced motion and turbulence in the airflow, and also with predictions from potential flow theory.

Phase and amplitude results for wave-related fluctuations are examined in detail and consistent departures from potential flow are noted. These departures are phase differences in between u and w which are not in quadrature, amplitudes of u and w which vary throughout the periods, and phase shifts of u and w which differ from those predicted by potential flow theory.

Conclusions for the role of turbulence in the interactions are based on JPDF-CMF and phase amplitude analyses.

DD FORM 1 NOV 65 1473 (PAGE 1)

S/N 0101-807-6811

Security Classification

A-31408

14 KEY WORDS	LINK A		LINK B		LINK C	
	ROLE	WT	ROLE	WT	ROLE	WT
Turbulence						
Wave-induced motion						
Observational data						
Potential flow predictions						
Wind-wave coupling						

Thesis
T437
c.1

135611

Thompson
Wave-related distur-
bances in the velocity
field over ocean waves.

Thesis
T437
c.1

135611

Thompson
Wave-related distur-
bance in the velocity
field over ocean waves.

thesT437
Wave-related disturbances in the velocit
3 2768 002 03508 1
DUDLEY KNOX LIBRARY